

# Reconciling grand unification with strings by anisotropic compactifications

Ben Dundee, Stuart Raby, and Akin Wingerter

*Department of Physics, The Ohio State University, 191 West Woodruff Avenue, Columbus, Ohio 43210, USA*

(Received 28 May 2008; published 11 September 2008)

We analyze gauge coupling unification in the context of heterotic strings on anisotropic orbifolds. This construction is very much analogous to effective five-dimensional orbifold grand unified theory field theories. Our analysis assumes three fundamental scales: the string scale  $M_s$ , a compactification scale  $M_c$ , and a mass scale for some of the vectorlike exotics  $M_{\text{ex}}$ ; the other exotics are assumed to get mass at  $M_s$ . In the particular models analyzed, we show that gauge coupling unification is not possible with  $M_{\text{ex}} = M_c$ , and in fact we require  $M_{\text{ex}} \ll M_c \sim 3 \times 10^{16}$  GeV. We find that about 10% of the parameter space has a proton lifetime (from dimension six gauge exchange)  $10^{33} \text{ yr} \lesssim \tau(p \rightarrow \pi^0 e^+) \lesssim 10^{36} \text{ yr}$ . The other 80% of the parameter space gives proton lifetimes below Super-Kamiokande bounds. The next generation of proton decay experiments should be sensitive to the remaining parameter space.

DOI: [10.1103/PhysRevD.78.066006](https://doi.org/10.1103/PhysRevD.78.066006)

PACS numbers: 11.25.Mj

## I. INTRODUCTION

Supersymmetric grand unification [1–6] is one of the most attractive scenarios for beyond the standard model physics. One can simultaneously explain the apparent unification of the electroweak and strong coupling constants around  $3 \times 10^{16}$  GeV, charge quantization, the conservation of baryon number minus lepton number (B-L), and why quarks and leptons come in families. Nevertheless the simplest four-dimensional supersymmetric (SUSY) grand unified theories (GUTs) have some notable problems. Spontaneously breaking the GUT symmetry requires scalars in adjoint representations and complicated symmetry breaking potentials. In addition, Higgs doublet-triplet splitting demands special treatment. Neither of these problems is insurmountable, but it is difficult to imagine that these special sectors can be derived from a more fundamental theory. In addition, Super-Kamiokande (Super-K) bounds on the proton lifetime place four-dimensional SUSY GUTs “under siege” [7,8]. Finally, in order to understand fermion masses and mixing angles it is likely that additional family symmetries may be needed.

In the early work within the framework of the weakly coupled heterotic string it was argued for string unification, as opposed to grand unification with an independent lower-energy GUT breaking scale.<sup>1</sup> Gauge couplings naturally unify at the string scale with a unification scale<sup>2</sup> of around  $5 \times 10^{17}$  GeV [9–11]. Unfortunately the precision low-energy data prefer a lower unification scale  $M_{\text{GUT}} \sim 3 \times 10^{16}$  GeV. This tension between gravity and gauge coupling unification has been termed the “factor of 20” problem with string unification [12]. Nevertheless string theory has some very nice features; i.e. the  $E_8 \times E_8$  [or  $SO(32)$ ]

symmetry of the weakly coupled heterotic string is easily broken via an orbifold compactification of the extra 6 spatial dimensions [13,14]. In addition, Higgs doublet-triplet splitting is also easily accomplished by the same means [15,16]. Significant progress was made early on in obtaining standard-model-like theories using orbifolding and Wilson lines to break the gauge symmetry [16–20].

More recently, it was realized that some of the problems with SUSY GUTs could be solved by understanding our low-energy physics in terms of an effective five- or six-dimensional field theory in which one or two of the directions is compactified [21–30]. Typically one takes a five- (six-) dimensional gauge theory and compactifies one (two) of the directions on an orbifold. The geometry of the orbifold admits solutions for higher-dimensional fields which are localized on two or more branes and fields which are free to propagate in the bulk. The former are called “brane” fields, the latter “bulk” fields. By assigning the bulk fields boundary conditions along the fifth (and sixth) direction(s), one can achieve GUT/SUSY breaking without the large representations and complicated GUT breaking potentials encountered in four-dimensional constructions. In addition, placing the electroweak Higgs multiplet in the bulk, Higgs doublet-triplet splitting can also be affected via a judicious choice of boundary conditions. Generally, the placement of the matter and the assignment of orbifold parities is done in a bottom-up manner; one identifies certain phenomenological features (e.g. suppressing dangerous proton decay operators) and then chooses mass scales, matter localization, and orbifold parities accordingly. For example, one can keep  $b - \tau$  Yukawa unification by placing the third family on an  $SU(5)$  brane or suppress proton decay by placing the first two families in the bulk [24]. Finally, four-dimensional SUSY GUTs require of order 3% threshold correction at the GUT scale in order to precisely fit the low-energy data [31]. Given a GUT breaking sector, this correction must come from the spectrum of massive states with mass of order  $M_{\text{GUT}}$ . In orbifold

<sup>1</sup>In fact, it is difficult to get massless adjoints in the string spectrum, needed for GUT symmetry breaking.

<sup>2</sup>Assuming  $SU(2)$  and  $SU(3)$  are represented at Kač-Moody level  $k_2 = k_3 = 1$  and the  $U(1)$  of hypercharge is normalized with  $k_1 = 5/3$ .

GUTs this correction comes from the Kaluza-Klein modes between the compactification scale  $M_C$  and the cutoff scale  $M_*$ , with unification occurring at the cutoff. In fact, the ratio  $M_*/M_C \sim 100$  is determined by gauge coupling unification. The problem with orbifold GUT field theories, however, is the necessity for a cutoff.

In Refs. [32–34], it was shown that effective orbifold SUSY GUT field theories can be obtained by orbifold compactifications of the heterotic string. These theories provide an ultraviolet completion of orbifold GUT field theories with a physical cutoff at the string scale. These are so-called anisotropic orbifold theories with one or two large extra dimensions ( $R = M_C^{-1} \gg l_s = M_s^{-1}$ ). At lowest order the gauge couplings unify at  $M_s$ . Further, when working within the framework of the weakly coupled heterotic string, there is a very specific relationship between the strength of the GUT coupling and the strength of gravity [see Eq. (2)]. Viewed in this manner, the factor of 20 turns into a factor of 400 when comparing to the (experimentally measured) value of Newton’s constant. This makes it clear that there need to be significant threshold corrections (both logarithmic and power-law) in order to match the low-energy data. In fact, important threshold corrections are provided by Kaluza-Klein modes running in loops. Their spectrum is calculable and often gives nontrivial corrections to the running of the couplings [21,22].

In this paper, we investigate ways to solve the “factor of 20” problem with heterotic string unification, within the context of the orbifold GUT picture proposed in Refs. [32–34].<sup>3</sup> In order to make unification work, we find that we generally need to introduce an intermediate scale  $M_{\text{ex}}$ , which is typically 2 or 3 orders of magnitude below the compactification scale. When we impose the conditions that  $M_s > M_C \geq M_{\text{ex}}$ , we find a large number of solutions for which unification works. Note the proton lifetime (from dimension six operators) scales as the fourth power of  $M_C$ . Most solutions are excluded by proton decay; however, a small number predict proton lifetimes (from dimension six operators) that can be measured in future experiments.

We begin with a brief review of the stringy embedding of orbifold GUTs [32–34] and a presentation of the models in the “mini-landscape” search [36–40] in Sec. II. We focus on two “benchmark” models from the mini-landscape search in this analysis, called “model 1A” and “model 2” in Ref. [40]. Specific details of these models (the full spectrum in four dimensions, etc.) can be found in Tables I, II, III, IV, V, VI, VII, VIII, and IX in Appendix C. The main result of our analysis is a detailed examination of the parameter space which allows for unification and how this parameter space relates to proton decay constraints from dimension six (and possibly dimen-

sion five) operators. This work is summarized in Sec. III. Solutions consistent with gauge coupling unification are found in Tables VII, VIII, and IX. In Sec. IV we check whether any of our solutions are consistent with decoupling of exotics in supersymmetric vacua.

## II. ORBIFOLD GUTS FROM STRING THEORY

In exploring gauge coupling unification in orbifold constructions, we focus on a class of models [36–40] that are based on SU(6) gauge-Higgs unification in five dimensions and whose low-energy spectrum is exactly that of the minimal supersymmetric standard model (MSSM). Similar theories have also been considered in the context of orbifold GUT field theory [42]. We shall comment on the differences in Appendix A.

### A. The mini-landscape in a nutshell

We compactify the six extra dimensions of the heterotic string on the product of three 2-tori as shown in Fig. 1. Modding out the discrete  $\mathbb{Z}_6$ -II symmetry given as a  $60^\circ$ ,  $120^\circ$ , and  $180^\circ$  rotation (“twist”  $v$ ) in the first, second, and third torus, respectively, defines the orbifold [13,14]. The geometry of the orbifold allows for no Wilson lines in the first torus, one order-3 Wilson line  $A_3$  in the second torus ( $e_3$  and  $e_4$  are the same direction on the orbifold) and two order-2 Wilson lines  $A_2$  and  $A'_2$  along  $e_5$  and  $e_6$ , respectively [43]. We take  $A'_2 \equiv 0$  to localize two identical copies of  $\mathbf{16}$ ’s at the fixed points  $\bullet$  and  $\star$  that will eventually sport a  $D_4$  family symmetry [34,44,45].

Modular invariance allows for 61 different gauge embeddings (“shift”  $V$ ) of the twist. Only 15 of these shifts break  $E_8 \times E_8$  to a gauge group containing SO(10), and only 2 shifts allow for  $\mathbf{16}$ ’s in the first/fifth twisted sector ( $T_1$  and  $T_5$ , respectively) that are not projected out by the Wilson lines.

The models that come closest to the real world all stem from one shift [36,37], termed  $V^{\text{SO}(10),1}$  in Refs. [39,40]. Switching on all possible Wilson lines consistent with this shift and modular invariance, we obtain  $\sim 22\,000$  models with different particle spectra. Successively, we impose our phenomenological priors to get as close to the MSSM as we possibly can: (i) standard model (SM) gauge group; (ii) nonanomalous hypercharge that lies in  $\text{SU}(5) \subset \text{SO}(10)$ ; (iii) 3 generations of quarks and leptons, 1 pair of Higgs doublets; (iv) all exotic (i.e. non-standard-model) particles are vectorlike; (v) trilinear Yukawa coupling for a heavy top; (vi) generalized B-L generator that is eventually broken down to  $R$  parity; (vii) all spurious Abelian gauge group factors are broken; (viii) string selection rules allow for all exotics to decouple consistent with the “choice of vacuum” [singlet vacuum expectation values (VEVs) must not break SM gauge symmetries and  $R$  parity and must satisfy  $F = D = 0$ ].

This leaves us with 15 models with promising phenomenology. We use this sample to investigate whether the

<sup>3</sup>A recent analysis of gauge coupling unification can also be found in Ref. [35].

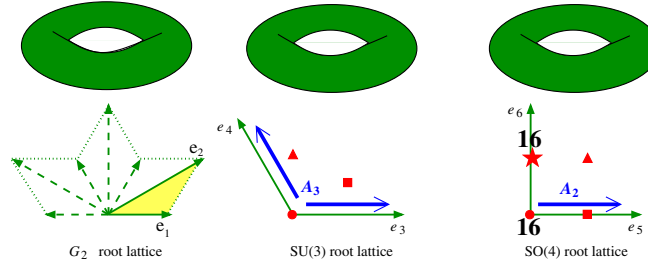


FIG. 1 (color online). The geometry of the compact dimensions.

unification picture in orbifolds is consistent with the measured values of the coupling constants at low energies or, in other words, whether we can fit  $\alpha_1$ ,  $\alpha_2$  and  $\alpha_3$  at the electroweak scale with a single coupling constant  $\alpha_{\text{STRING}}$  at  $M_s$ . Specifically, the set of exotics in both models 1 and 2 of Ref. [40] are similar enough to warrant parallel treatment and are listed in Table IV in Appendix C. As can be seen, the exotic matter which is charged under the MSSM in model 1 overlaps with the exotic matter in model 2. Note that we have labeled states with their hypercharge and B-L quantum numbers as subscripts.

### B. The orbifold GUT picture

The 15 models described in Sec. II A are naturally embedded into a grand unified theory in five or six dimensions [32]. Consider model 2 of Sec. 5.2 of the minilandscape search [40]. For completeness, the full details of the model have been reproduced in Appendix C.

Instead of modding out the full  $\mathbb{Z}_6 - \Pi \simeq \mathbb{Z}_2 \times \mathbb{Z}_3$  symmetry (generated by the twist  $\nu$ ) to get the four-dimensional spectrum, we can mod out the  $\mathbb{Z}_3$  subgroup (generated by  $2\nu$ ) alone, leaving the  $\text{SO}(4)$  torus invariant. The particles from the  $U$ ,  $T_2$ , and  $T_4$  sectors are free to move around in the  $\text{SO}(4)$  torus and can thus be considered to be the “bulk states” of a six-dimensional  $\mathbb{Z}_3$  orbifold with twist  $2\nu$ , shift  $2V$  and Wilson line  $A_3$ .

In this picture, modding out the residual  $\mathbb{Z}_2$  symmetry (generated by  $3\nu$ ) corresponds to adding “brane states” to the theory. The gauge group at the fixed points is obtained from the bulk symmetry by modding out  $V_2 = 3V$  for  $\bullet$  and  $\star$  and  $V_2 + A_2$  for  $\blacksquare$  and  $\blacktriangle$ . The matter representations follow from the mass equation at the respective fixed points (given in terms of  $V_2$  and  $A_2$ ), subject to projection conditions from  $V_3 = 2V$  and  $A_3$ .

The gauge symmetry in four dimensions is the intersection of all gauge groups, and the brane GUT states branch to SM representations of the  $T_1$ ,  $T_3$ , and  $T_5$  sectors. This can be understood from an orbifold GUT viewpoint by assigning parities to the brane modes given by

$$P \sim e^{2\pi i p \cdot V_2}, \quad P' \sim e^{2\pi i p \cdot (V_2 + W_2)},$$

where  $p$  (the highest weight associated with the state) is a sixteen-dimensional vector from the  $E_8 \times E_8$  lattice. Then, the setup of Fig. 2 describes an orbifold  $S^1/\mathbb{Z}_2 \times \mathbb{Z}'_2$  where

1 extra dimension is compactified on a circle. The discrete symmetries are realized as a reflection  $\mathcal{P}: x^5 \rightarrow -x^5$  and a translation  $\mathcal{T}: x^5 \rightarrow x^5 + 2\pi R$ . Only the states that are invariant under

$$\begin{aligned} \mathcal{P}: \Phi(x^5) &\rightarrow \Phi(-x^5) = P\Phi(x^5), \\ \mathcal{PT}: \Phi(x^5) &\rightarrow \Phi(-x^5 + 2\pi R) = P'\Phi(x^5) \end{aligned} \quad (1)$$

will be present in the low-energy spectrum.<sup>4</sup>

Orbifold GUTs, when generated from an underlying string theory, are significantly more constrained than orbifold GUT field theories. Whereas the only *real* constraint in an orbifold GUT field theory is that the low-energy effective field theory be anomaly-free, all anomalies in the string theory are canceled at the string scale by the generalized Green-Schwarz mechanism [46–50], so this condition is automatically satisfied. In string orbifolds, the parities are realized in terms of Wilson lines that must satisfy stringent modular invariance constraints, so we cannot simply assign parities at will. Further, the placement of matter is not an independent degree of freedom in string models. Finally, we are given a value for the coupling constant at the cutoff; see Eq. (2). In a typical orbifold GUT, this is a free parameter. In addition, there may be some assumptions about strong coupling, but the details of the ultraviolet completion are not addressed.

## III. GAUGE COUPLING UNIFICATION IN ORBIFOLDS

### A. Unification in heterotic string theory in 10 dimensions

As a unified framework for particle physics and gravity, string theory predicts Newton’s constant  $G_N$  and relates it to the gauge coupling constants. Unfortunately, the predicted value for  $G_N$ , in the weakly coupled heterotic string, turns out to be too large and needs to be reconciled with the extrapolated running gauge coupling constants at the unification scale.

Throughout this paper we assume that we are in the weakly coupled regime of the heterotic string. After compactifying the ten-dimensional low-energy effective action

<sup>4</sup> $P' \equiv PT$ , where  $T$  corresponds the discrete gauge transformation due to a Wilson line.

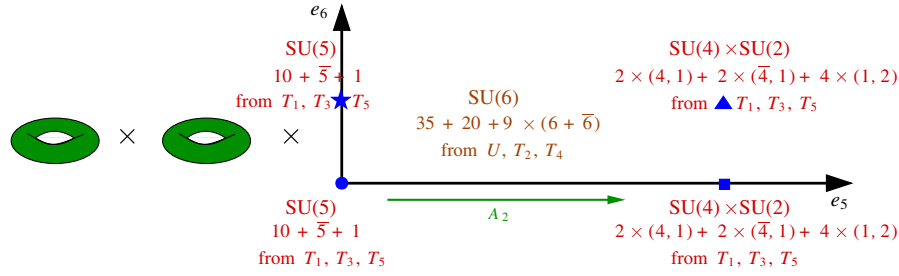


FIG. 2 (color online). Setup of the 5D orbifold GUT, where the fifth dimension ( $e_5$ ) is large compared to the other compact dimensions.

on a six-dimensional manifold, one obtains [9]

$$G_N = \frac{1}{8} \alpha_{\text{STRING}} \alpha'. \quad (2)$$

Here,  $\alpha_{\text{STRING}}$  denotes the common value of the gauge coupling constants at the string scale  $M_s = 1/\sqrt{\alpha'}^{1/2}$ . Low-energy data suggest  $\alpha_{\text{STRING}}^{-1} \approx \alpha_{\text{GUT}}^{-1} \approx 24$  and  $M_s \approx M_{\text{GUT}} \approx 10^{16}$  GeV, so the predicted value for Newton's constant is off by a factor of about 400. Putting it another way, if we use the measured value of the gravitational constant  $G_N = 1/(M_{\text{PL}}^2)$  with  $M_{\text{PL}} \approx 1.2 \times 10^{19}$  GeV, the string scale is predicted to be  $M_s \approx 5 \times 10^{17}$  GeV [9], in disagreement with  $M_{\text{GUT}}$ . These conclusions are based on the assumptions that (i) we are in the weak coupling limit, (ii) there are no new states between the electroweak and the GUT scale that could contribute to the renormalization group equations (RGEs), and (iii) the compactification is isotropic; i.e. all compactified dimensions are comparable in size.

In the following, we explore *anisotropic orbifold compactifications* to fit low-energy data with a single coupling constant at  $M_s$ .<sup>6</sup> Other proposals that have been considered in the literature include exotic matter representations at intermediate scales, large threshold corrections, nonstandard hypercharge normalizations from higher-level Kač-Moody algebras, strings without supersymmetry, or the strong coupling regime of the heterotic string [9–11, 35, 54]. For a review of grand unification in the context of string theory, see Ref. [12].

## B. The RGEs for anisotropic orbifold compactifications

We study gauge coupling unification for the benchmark models presented in the mini-landscape search [40]. As has been emphasized in Sec. II A, these models are 2 out of 15 that already satisfy quite a few nontrivial criteria on the road to the MSSM. We are working in the orbifold GUT limit as outlined in Sec. II B. The gauge group geography and the relevant part of its five-dimensional spectrum for model 2 are given in Fig. 2. For the full details of the four-

dimensional spectrum, see Tables I and II in Appendix C. The anisotropic compactification singles out the fifth dimension that is assumed to be large and thus introduces a new scale into the theory, the compactification scale  $M_C$ . The other five compactified dimensions are assumed to be of order the string scale  $M_s$ .

We want to compare our models with low-energy data. At the string scale  $M_s$ , we have a unified gauge coupling  $\alpha_{\text{STRING}}$ . Below the string scale we have three gauge couplings which renormalize independently down to the weak scale. In general, there are additional small (stringy) corrections to the relationship in Eq. (2) at the string scale  $M_s$  [9–11]. Because these contributions are expected to be small, we will neglect them in this analysis. In principle we should integrate the three gauge couplings down to the SUSY breaking scale using the two-loop RGEs, including one-loop threshold corrections at the string scale, the compactification scale, the exotic scale,  $M_{\text{EX}}$ , and the SUSY scale, finally fitting  $\alpha_i$ ,  $i = 1, 2, 3$ , at  $M_Z$  [55, 56]. However, it is sufficient to compare the orbifold GUT to the four-dimensional SUSY GUT running equations, which approximately (and implicitly) correct for SUSY threshold corrections at the weak scale and two-loop renormalization group running from the weak scale to the GUT scale. These are given by the equations

$$\alpha_i^{-1}(\mu) = \alpha_{\text{GUT}}^{-1} + \frac{b_i}{2\pi} \log \frac{M_{\text{GUT}}}{\mu} + \frac{6}{2\pi} \delta_{i3}. \quad (3)$$

The indices  $i = 3, 2, 1$  refer to  $\text{SU}(3)_c$ ,  $\text{SU}(2)_L$ , and  $\text{U}(1)_Y$ , respectively. The  $b_i$  are the so-called  $\beta$ -function coefficients and are most conveniently expressed in terms of the Dynkin index<sup>7</sup> [57]

$$b_i = -3\ell(\text{vector multiplets}) + \ell(\text{chiral multiplets}). \quad (4)$$

For the MSSM we have  $b_i = (-3, 1, 33/5)$ . Finally, the last term in Eq. (3) is a 3% threshold correction to  $\alpha_3^{-1}$  at the GUT scale that we need to match the precision electroweak data.

<sup>5</sup>The string scale  $M_s$  defined here corresponds to the effective cutoff scale in our field theory calculation. This is discussed in more detail in footnote <sup>8</sup>, Sec. III B.

<sup>6</sup>For earlier work along this line, see [34, 51–53].

<sup>7</sup>For hypercharge, we define the Dynkin index to be  $\ell = (3/5)Y^2/4$ .



The minimal and most elegant way to fit the low-energy data is to arrange for all exotics (i.e. non-standard-model particles) to obtain mass around  $M_s$ . Up to the scale  $M_C$ , assumed to be not much below  $M_{\text{GUT}}$ , the evolution of the gauge coupling constants is then governed by the same renormalization group equations as in the usual GUT picture. For energies above  $M_C$ , the RGEs receive additional contributions from the Kaluza-Klein tower of those standard model particles that live in the bulk, thus giving rise to both logarithmic and power-law running [21,22]. Unfortunately, this simple setup does not work. Varying the values of  $\alpha_{\text{STRING}}$  at  $M_s$  and of the compactification scale  $M_C$ , we cannot fit the gauge coupling constants at the electroweak scale. We elaborate on this point in Appendix A, where we show the difficulties involved with gauge-Higgs unification in five dimensions.

The remaining possibility is to assume that not all exotics obtain mass at  $M_s$ , but some are light enough to be relevant for the evolution of the coupling constants. At the same time, of course, the exotics must still be massive enough to decouple from the low-energy theory. We will call this intermediate scale  $M_{\text{EX}}$  and assume in the following  $M_s > M_C \gtrsim M_{\text{EX}}$ . Now we can try to fit the low-energy data by varying  $M_{\text{EX}}$ ,  $M_C$ ,  $M_s$  and the multiplicities and quantum numbers of the light exotics. Note that the running of the coupling constants below  $M_{\text{EX}}$  will be given by the same Eq. (3) as in the MSSM, since all of the exotics are assumed to be heavier than  $M_{\text{EX}}$  and the first excitation of the Kaluza-Klein (KK) tower is of order  $M_C$ . Near  $\mu \simeq M_{\text{EX}}$ , the renormalization group equations read:

$$\begin{aligned} \alpha_i^{-1}(\mu) = & \alpha_{\text{STRING}}^{-1} + \frac{b_i^{\text{MSSM},++} + b_i^{\text{MSSM,brane}}}{2\pi} \log \frac{M_s}{\mu} \\ & + \frac{b_i^{\text{EX},++} + b_i^{\text{EX,brane}}}{2\pi} \log \frac{M_s}{M_{\text{EX}}} - \frac{1}{4\pi} (b_i^{\text{MSSM},++} \\ & + b_i^{\text{MSSM},--} + b_i^{\text{EX},++} + b_i^{\text{EX},--}) \log \frac{M_s}{M_C} \\ & + \sum_{P=\pm, P'=\pm} \frac{b_i^{\text{MSSM},PP'} + b_i^{\text{EX},PP'}}{2\pi} \left( \frac{M_s}{M_C} - 1 \right). \quad (5) \end{aligned}$$

These equations are obtained by starting at the highest scale in the theory,  $M_s$ , and evolving the gauge couplings  $\alpha_i$  down to  $M_C$ , taking into account all of the particles with mass less than  $M_s$ . In the next step, one takes the values obtained for  $\alpha_i$  as boundary conditions for the renormalization group equations at  $M_C$  and calculates  $\alpha_i$  at  $M_{\text{EX}}$ . In order to compare to experimental values of the coupling constants at  $M_Z$ , we apply the two-loop RGEs [58]. Note that this involves integrating out SUSY particles at  $M_{\text{SUSY}}$ . Technically, because the two-loop RGEs are good *near* the GUT scale, our approach will be to compare the two equations [Eqs. (3) and (5)] at the scale  $M_{\text{EX}}$ . Provided that  $M_{\text{EX}}$  is near the GUT scale, the error introduced in the analysis should be negligible. In principle, the exotic scale

$M_{\text{EX}}$  can be small, perhaps a TeV. In all cases we find, however, the exotic scale is larger than  $10^9$  GeV, and in most cases it is greater than  $10^{12}$  GeV. The error we make by matching Eqs. (3) and (5) at  $M_{\text{EX}} \sim 10^9$  GeV comes from the difference in the two-loop corrections to the RG running from  $M_{\text{EX}}$  to the GUT scale. This correction is expected to be less than a percent.

Let us look at Eq. (5) in some more detail. The first term is the tree level boundary condition from the heterotic string. The second and third terms contain loop contributions from MSSM fields and exotic matter, respectively—the zero KK modes and the brane states are kept separate for clarity. The last two terms are due to the massive KK states in the bulk. The logarithmic ( $\sim \log \frac{M_s}{M_C}$ ) and linear ( $\sim \frac{M_s}{M_C}$ ) terms are a consequence of the geometry; i.e. in an equivalent string calculation the factor of  $\frac{M_s}{M_C}$  arises from the dependence on the  $T$  (volume) and  $U$  (shape) moduli of the torus.<sup>8</sup> Note that the last term is a universal correction due to the SU(6) fields in the bulk. We introduce the following definitions:

$$\begin{aligned} b_i^{\text{MSSM}} & \equiv b_i^{\text{MSSM},++} + b_i^{\text{MSSM,brane}}, \\ b_i^{\text{EX}} & \equiv b_i^{\text{EX},++} + b_i^{\text{EX,brane}}, \\ b_i^{++} & \equiv b_i^{\text{MSSM},++} + b_i^{\text{EX},++}, \\ b_i^{--} & \equiv b_i^{\text{MSSM},--} + b_i^{\text{EX},--}, \\ b^{\mathcal{G}} & \equiv \sum_{P=\pm, P'=\pm} b_i^{\text{MSSM},PP'} + b_i^{\text{EX},PP'}. \end{aligned}$$

This simplifies Eq. (5) a bit:

$$\begin{aligned} \alpha_i^{-1}(\mu) = & \alpha_{\text{STRING}}^{-1} + \frac{b_i^{\text{MSSM}}}{2\pi} \log \frac{M_s}{\mu} + \frac{b_i^{\text{EX}}}{2\pi} \log \frac{M_s}{M_{\text{EX}}} \\ & - \frac{1}{4\pi} (b_i^{++} + b_i^{--}) \log \frac{M_s}{M_C} + \frac{b^{\mathcal{G}}}{2\pi} \left( \frac{M_s}{M_C} - 1 \right). \quad (6) \end{aligned}$$

### C. Gauge coupling unification: An effective field theory calculation

Before we proceed, we will clear up some notational issues. We will *always* talk about fields in the language of

<sup>8</sup>Note that our one-loop calculations are performed using an effective field theory approach. In particular the sum over the infinite tower of KK modes follows the regularization scheme of Dienes, Dudas, and Gherghetta [21,22]. Moreover, in the work of Ghilencea and Nibbelink [59] it is shown that if the field theory cutoff  $\Lambda^2$  is chosen to satisfy the relation  $\Lambda^2 = \frac{2e}{3\sqrt{3}} \times \frac{1}{\alpha'} \approx 1.05/\alpha'$ , then the heterotic string loop calculation is approximately equal to the field theory results. Thus we identify the string scale  $M_s = \Lambda \approx \frac{1}{\sqrt{\alpha'}}$ . We should note that the analysis of [59] was done in the context of toroidal compactification. A more relevant comparison should be done in an orbifold compactification with Wilson lines. The latter approach was taken by the authors of Ref. [35] in a  $T^2/\mathbb{Z}_3$  orbifold. Their results, however, are not directly applicable to our situation.

$N = 1$  SUSY in four dimensions. The  $N = 1$ , 5-dimensional hypermultiplet contains two four-dimensional chiral multiplets, and a five-dimensional vector multiplet contains a four-dimensional vector multiplet and a four-dimensional chiral multiplet. The five-dimensional  $N = 1$  theory can thus be described in terms of four-dimensional  $N = 1$  fields (or in terms of four-dimensional  $N = 2$  hypermultiplets).

In order to check gauge coupling unification, we will equate the values of (i)  $1/\alpha_3 - 1/\alpha_2$ , (ii)  $1/\alpha_2 - 1/\alpha_1$ , and (iii)  $\alpha_3$  as obtained from Eqs. (3) and (6), respectively, at the scale  $M_{\text{EX}}$ , where both equations are valid. We find

$$\log \frac{M_s}{M_{\text{GUT}}} = \frac{n_3 - n_2}{4} \log \frac{M_s}{M_{\text{EX}}} - \frac{3}{2}, \quad (7a)$$

$$\log \frac{M_s}{M_{\text{GUT}}} = \frac{10n_2 - n_3 - 3n_1}{56} \log \frac{M_s}{M_{\text{EX}}} + \frac{3}{7} \log \frac{M_s}{M_c}, \quad (7b)$$

$$48\pi = \frac{\pi}{4} \left( \frac{M_{\text{PL}}}{M_s} \right)^2 - 6 - 3 \log \frac{M_s}{M_{\text{GUT}}} + n_3 \log \frac{M_s}{M_{\text{EX}}} + \log \frac{M_s}{M_c} - 4 \left( \frac{M_s}{M_c} - 1 \right), \quad (7c)$$

where the  $n_i$  are beta function contributions from the *brane-localized* exotics, as defined below. The first two equations describe the *relative* running of the couplings (i.e. their slopes), and the last one gives us information about the *absolute* running (i.e. their intercepts). The coefficients  $n_i$  are defined in terms of the set of exotics with mass of order  $M_{\text{EX}}$  as follows:

$$n_3 \times [(3, 1)_{1/3,*} + (\bar{3}, 1)_{-1/3,*}] + n_2 \times [(1, 2)_{0,*} + (1, 2)_{0,*}] + n_1 \times [(1, 1)_{1,*} + (1, 1)_{-1,*}], \quad (8)$$

where “\*” for the B-L charge denotes anything. The necessary  $\beta$ -function coefficients  $b_i$ , using the numbers in Table V in Appendix C, are found to be

$$\vec{b}_{\text{EX}} = \left( n_3, n_2, \frac{n_3 + 3n_1}{10} \right). \quad (9)$$

Let us now consider those MSSM states located in the bulk. In general, we can find two pairs of  $N = 1$  chiral multiplets  $\mathbf{6} + \mathbf{6}^c$  which decompose as

$$\begin{aligned} 2 \times (\mathbf{6} + \mathbf{6}^c) \supset & [(1, 2)_{1,1}^{--} + (\bar{3}, 1)_{-2/3,1/3}^{++}] \\ & + [(1, 2)_{-1,-1}^{++} + (\bar{3}, 1)_{2/3,-1/3}^{--}] \\ & + [(1, 2)_{1,1}^{--} + (\bar{3}, 1)_{-2/3,1/3}^{++}] \\ & + [(1, 2)_{-1,-1}^{++} + (\bar{3}, 1)_{2/3,-1/3}^{--}]. \end{aligned} \quad (10)$$

This gives us the third family  $\bar{b}$  and  $L$ —the rest of the third family comes from the  $\mathbf{10} + \mathbf{10}^c$  of SU(5) contained in the  $\mathbf{20} + \mathbf{20}^c$  of SU(6), which lives in the untwisted sector. An interesting point is the genesis of the Higgs bosons. We

have remarked earlier that the models we look at come from a broader class of models satisfying “gauge-Higgs unification.” Our bulk gauge symmetry is SU(6), so the SU(6) gauge bosons (and thus the adjoint representation) necessarily live in the bulk. Under  $\text{SU}(5) \times \text{U}(1)$ , the adjoint decomposes as

$$\mathbf{35} \rightarrow \mathbf{24}_0 + \mathbf{5}_{+1} + \mathbf{5}_{-1}^c + \mathbf{1}_0. \quad (11)$$

Thus the MSSM Higgs sector emerges from the breaking of the SU(6) adjoint by the orbifold. Including the contributions from the third family and the Higgses, we find using Table VI in Appendix C

$$\vec{b}^{++} = (-7, -3, 13/5), \quad \vec{b}^{--} = (5, 1, 1/5), \quad b^G = -4. \quad (12)$$

## D. Results

We find it necessary to introduce an intermediate mass scale  $M_{\text{EX}}$ , perhaps near the compactification scale, and identify a set of exotics with mass  $M_{\text{EX}}$  consistent with gauge coupling unification. Solving the RG equations numerically, we find 252 versions of model 2 (of which 82 are also versions of model 1), where by “versions” we mean inequivalent sets of “light” exotics satisfying gauge coupling unification. Of these 252 (82), only 48 (9) are consistent with the Super-K bounds on the proton lifetime [31] (see Sec. 3.5). These are found in Tables VII and VIII in Appendix C, where we also calculate the lifetime of the

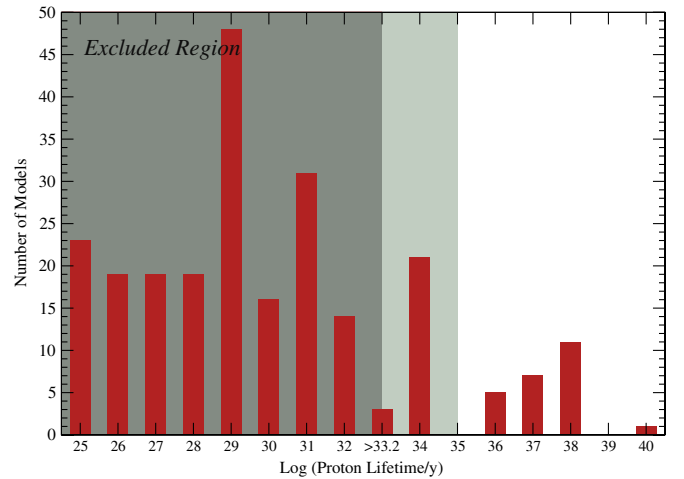


FIG. 3 (color online). Histogram of solutions with  $M_s > M_c \gtrsim M_{\text{EX}}$ , showing the models which are excluded by Super-K bounds (darker green) and those which are potentially accessible in a next generation proton decay experiment (lighter green). Of 252 total solutions, 48 are not experimentally ruled out by the current experimental bound, and most of the remaining parameter space can be eliminated in the next generation of proposed proton decay searches.

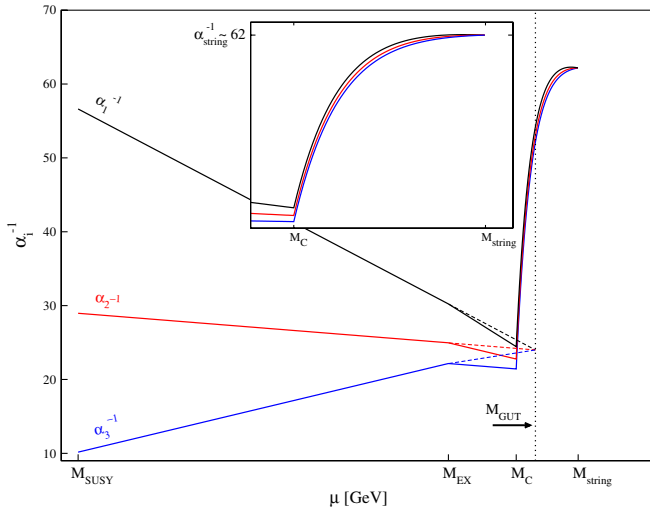


FIG. 4 (color online). An example of the type of gauge coupling evolution we see in these models versus the typical behavior in the MSSM. The “tail” is due to the power-law running of the couplings when towers of Kaluza-Klein modes are involved. Unification in this model occurs at  $M_s \approx 5.5 \times 10^{17}$  GeV, with a compactification scale of  $M_C \approx 8.2 \times 10^{15}$  GeV and an exotic mass scale of  $M_{EX} \approx 8.2 \times 10^{13}$  GeV.

proton due to dimension six operators; see Appendix B and Fig. 3. The solutions which are applicable to model 1 are listed in *bold* in both tables. Note that the GUT coupling constant  $\alpha_{\text{STRING}}$  (evaluated at  $M_s$ ) varies depending on  $M_s$  and  $M_{EX}$ . For example, in the last row of Table VII in Appendix C, we find

$$\alpha_{\text{STRING}}^{-1} = \frac{1}{8} \left( \frac{M_{\text{PL}}}{M_s} \right)^2 \approx \frac{1}{8} \left( \frac{1.22 \times 10^{19} \text{ GeV}}{5.47 \times 10^{17} \text{ GeV}} \right)^2 \approx 62. \quad (13)$$

Near the exotic scale where we match onto the low-energy physics, we expect the (inverse) coupling constants to be of order 30–40. Likewise,  $\alpha_{\text{STRING}}^{-1}$  is typically *larger* than this, of order 50–60 or so [but sometimes as big as  $\mathcal{O}(1000)$ ]. Thus, we *must* have a large and negative contribution from the power-law running, which translates into the requirement that  $b^{\mathcal{G}} < 0$ . This is evident in Eq. (6), for example. If  $b^{\mathcal{G}} > 0$ , we would need a large negative contribution from the other terms, which is hard to reconcile with the logarithmic suppression. For completeness, we plot the  $\beta$  functions of the last solution in Table VII in Fig. 4. The evolution of the gauge couplings is typical in this class of models; i.e. the power-law running between the compactification scale is rather pronounced.

For the 11 models in Table VII, we keep only the minimum amount of matter in the bulk; i.e. in order to get the MSSM spectrum, it is sufficient to keep  $2 \times (\mathbf{6} + \mathbf{6}^c)$  massless below the string scale. Given the constraint that we want  $b^{\mathcal{G}} < 0$ , however, we are in principle able to leave  $4 \times (\mathbf{6} + \mathbf{6}^c)$  massless below the string scale. This

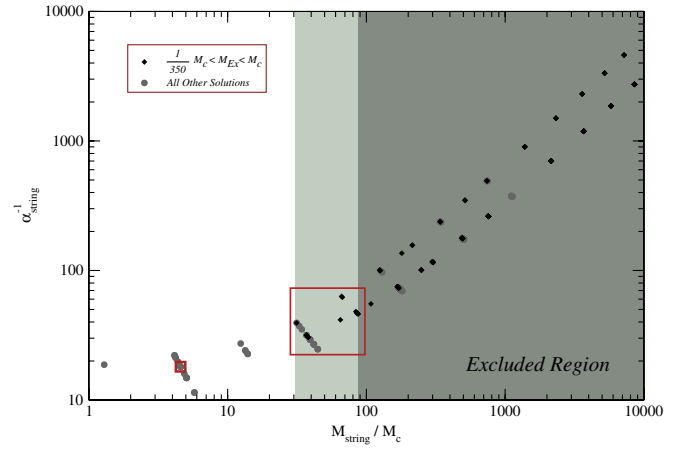


FIG. 5 (color online). Here we show the correlation between the hierarchies in the problem. Quite generally, a small value of  $\alpha_{\text{STRING}}^{-1}$  requires a large hierarchy between the compactification scale and the exotic scale. Again we show the excluded (darker green) and possibly testable (lighter green) models. The exact relationship between the ratio of  $M_s/M_C$  and the proton lifetime is given in Appendix B. In particular, note the “nice” models (black diamonds) in the large red box, characterized by moderate hierarchies between all scales. These models are collected in Table IX. Finally, note the one point in the small red box—this model is described in Sec. IV.

gives  $b^{\mathcal{G}} = -2$  and leads to 37 new solutions. These are listed in Table VIII in Appendix C. Of the 48 solutions (included in both models 1 and 2), 22 have proton lifetimes which can potentially be tested by the next generation of proton decay experiments; see Appendix B and Fig. 3 for more details.

We stress that this analysis is quite general. Of the 15 models which fit the criteria in the mini-landscape search, all come from a five-dimensional  $SU(6)$  orbifold, and all of them have the same types of exotics. This means that the analysis performed here generalizes in a straightforward manner to the other mini-landscape models, whose spectra are listed in Ref. [60].

In order to try and get a feel for the tunings involved in the above conclusions, we can compare the GUT coupling constant (at the string scale) with the ratio between the string scale and the compactification scale.<sup>9</sup> Further, we will separate the solutions based on the hierarchy between the compactification scale and the exotic scale. We plot the result in Fig. 5. What we see is the correlation between a long-lived proton and a moderate hierarchy between the compactification scale and the string scale and between the string scale and the Planck scale. However, these moderate hierarchies come at the cost of introducing a smaller and smaller exotic scale  $M_{EX}$ . This means that a long-lived proton favors a *large* hierarchy between the compactifica-

<sup>9</sup>The proton decay rate  $\Gamma(p \rightarrow \pi^0 e^+)$  is proportional to the fourth power of the GUT coupling constant; see Appendix B.

tion scale and the exotic scale. The black diamonds represent those models with a moderate [ $< \mathcal{O}(350)$ ] hierarchy between the compactification scale and the exotic scale. Most of these solutions are already ruled out by proton decay constraints. The gray shaded circles represent those solutions for which there is a large difference between the exotic scale and the compactification scale.

We would also like to point out the small set of solutions in the large red box, for which there are only moderate hierarchies and which are consistent with the current bounds on dimension six operators.<sup>10</sup> Specifically, there seems to be a “sweet spot” where all of the hierarchies in the problem are of  $\mathcal{O}(100)$  or so. These models are highlighted in Table IX. In particular, these models can all be eliminated by improving the current bounds on proton decay from dimension six operators by a factor of 50–100.

The fact that the data fall approximately on two straight lines is not surprising and is evidence of a power-law relationship between  $\alpha_{\text{STRING}}^{-1}$  and  $\frac{M_s}{M_c}$ . One can see this relationship by eliminating  $\log \frac{M_s}{M_{\text{EX}}}$  between Eqs. (7a) and (7b). We eventually find

$$\log \alpha_{\text{STRING}}^{-1} = A \log \frac{M_s}{M_c} + B, \quad (14)$$

where  $A$  and  $B$  are given in terms of the beta function coefficients and  $\log \frac{M_{\text{PL}}}{M_{\text{GUT}}}$ . It is not surprising to find that the actual values for  $A$  and  $B$  are roughly the same for all of the solutions and that many solutions give *identical* values for  $A$  and  $B$ .

#### IV. UNIFICATION, DECOUPLING OF EXOTICS AND SUPERSYMMETRY

Now that we understand what exotic matter we need to accommodate unification, we can ask if an intermediate scale  $M_{\text{EX}}$  is consistent with decoupling of the other exotics. The potential difficulty can be summarized as follows: all of the  $(200\,000 +)$  mass terms in the superpotential come from giving various MSSM singlets VEVs. Above, we have shown that unification depends on some exotics receiving mass at the string scale and some exotics receiving mass at an intermediate scale. This means that some singlets need to have VEVs on the order of the string scale  $M_s$ , while other singlets need to have VEVs on the order of the exotic mass scale  $M_{\text{EX}}$ . It is not obvious, *a priori*, that we can do this in a consistent way. That is, decoupling with  $D = F = 0$  was checked in Ref. [40] but only for the case where all of the singlet VEVs were of order the string scale. In light of gauge coupling unification, we are motivated to revisit the previous conclusions.

As we will show, there is a very nice way to accommodate unification in model 1A, which relies only on moderate tunings. The tunings will be apparent when we address the question of  $F = 0$ . We will see how some numbers of order the string scale must conspire to cancel some numbers of order the exotic scale.

While models 1A and 2 have similar sets of exotics, *they have different superpotentials*. So while it is possible to find nice ways to accommodate unification within model 1A, we find that there *does not* seem to be an easy way to assign singlet VEVs in model 2 such that we can accommodate unification. This does not mean that it is impossible to accommodate unification in model 2, but it does make the process of assigning singlet VEVs an exercise in fine-tuning.

In what follows, we use the notation defined in Ref. [40] concerning the MSSM singlets. In short, the states labeled  $s_i$  are singlets under the hidden sector and visible sector gauge groups, while the states labeled  $h_i$  transform as (hidden sector) SU(2) doublets. Some subset of the  $s_i$  and  $h_i$  are expected to get nonzero VEVs, which defines a vacuum configuration. Again, we refer the reader to Ref. [40] for more details.

#### A. Model 1A

Let us first consider the issue of unification in model 1A, where we can solve the  $F_i = 0$  equations exactly, giving us conditions on the singlet VEVs to ensure that mass terms for the exotics do not break supersymmetry at some high scale. We must check that we can consistently give some exotics intermediate scale mass, while maintaining supersymmetry.

It turns out that giving only brane-localized exotic matter intermediate scale mass will not give gauge coupling unification in this model. This can be seen as follows: in order to get unification, we need  $b_3^{\text{EX}} - b_2^{\text{EX}} > 0$ ; otherwise, the prediction for the string scale is  $M_s \lesssim 10^{15}$  GeV. The states which contribute to this difference are (see Table IV, for example)

$$\begin{aligned} v &\equiv (\mathbf{3}, 1)_{1/3, -2/3}, \\ m &\equiv (\mathbf{1}, \mathbf{2})_{0,*}, \quad \text{and} \quad y \equiv (\mathbf{1}, \mathbf{2})_{0,0}. \end{aligned} \quad (15)$$

The mass matrices for the  $y$  and  $v$  turn out to be the same, which means that we always get an equal number  $v + \bar{v}$  and  $y + \bar{y}$  with the same mass. One can check in Table VII that there are no solutions in which the number of  $v + \bar{v}$  is less than or equal to the number of  $y + \bar{y}$ . Conversely, one can see this from Eq. (7a). If  $n_2 \geq n_3$ , the string scale must be smaller than the GUT scale (assuming  $M_s > M_{\text{EX}}$ ), which (as we have previously argued) is not physical. Thus we *must* give some bulk exotic matter intermediate scale mass as well.

In giving bulk matter mass, we are severely limited in our options. For one, the requirement that  $b^{\mathcal{G}} < 0$  means

<sup>10</sup>See Appendix B for more details.



that we can keep only two extra pairs of  $\mathbf{6} + \mathbf{6}^c$  light. Further, there is only one pair of extra down quarks and the states  $\delta + \bar{\delta}$ . In the first case, the extra  $d + \bar{d}$  pair comes in an SU(6) multiplet with an extra  $\ell + \bar{\ell}$ , both of which have  $(++)$  boundary conditions and both of which couple in the same way to the singlet fields (to sixth order, and likely to all orders). This means that they must get the same mass, and we cannot get  $b_3^{\text{EX}} - b_2^{\text{EX}} > 0$  in this manner. The remaining option is that we find an assignment of singlet VEVs to give one pair of  $\delta + \bar{\delta}$  intermediate scale mass.

Let us be a bit more explicit about how one would accomplish this, starting with a brief examination of the  $\delta$ 's. The mass matrix for the  $\delta$ 's looks like

$$\mathcal{M}_{\delta\bar{\delta}} = \begin{pmatrix} 0 & B_1 & B_2 & 0 & 0 & 0 \\ B_3 & A_1 & A_2 & 0 & 0 & 0 \\ B_4 & A_3 & A_4 & 0 & 0 & 0 \\ 0 & 0 & 0 & C_1 & C_2 & D_1 \\ 0 & 0 & 0 & C_3 & C_4 & D_2 \\ 0 & 0 & 0 & D_3 & D_4 & 0 \end{pmatrix}, \quad (16)$$

where  $A_i, B_i, C_i$  and  $D_i$  are functions of singlet fields. Let us concentrate on the upper left block of this matrix, which involves only  $A_i$  and  $B_i$ . (The expressions for  $C_i$  and  $D_i$  are long and unenlightening and are not essential for the discussion here.) In general, the entries in the matrix have the following form:

$$A_i \sim \frac{1}{M_s^5} s_1 \cdot s_5 \cdot s_6 \cdot s_{18} \cdot (h_1 \cdot h_{10} + h_2 \cdot h_9), \quad (17)$$

$$B_i \sim \frac{1}{M_s^5} s_5 \cdot s_6 (h_{10} \cdot h_1 + h_9 \cdot h_2) \cdot (h_1 \cdot h_2 + s_{17} \cdot s_{18}). \quad (18)$$

Naively, diagonalizing this block gives one zero eigenvalue, which means that there are two linear combinations of the  $\delta$ 's that are massless. However, one must remember that the string selection rules give us only the *form* of the Yukawa couplings and not their exact magnitudes. In general, this means that we should be calculating  $N$  point correlation functions on the orbifold in order to get the *exact* Yukawa couplings in the theory. In particular, it is important to remember that the  $\delta$ 's live at *different* orbifold fixed points, and the interaction eigenstates are a linear superposition of these ‘‘orbifold eigenstates.’’ Returning to Eq. (17), we see that if we require

$$\langle s_1 \rangle \sim M_{\text{EX}}, \quad \text{all other singlets} \sim M_s, \quad (19)$$

we naturally get one eigenstate with mass of order  $M_{\text{EX}}$  and five heavy ( $\sim M_s$ ) eigenstates. We note that there is some dependence on  $\langle s_1 \rangle$  in the  $C_i$  and  $D_i$  at fifth order in the singlets; however, there is *no* dependence at sixth order, suggesting that these terms (in general) dominate the much smaller fifth-order terms.

Next we consider the  $\nu + \bar{\nu}$  and  $y + \bar{y}$ . The mass matrices for these states are  $2 \times 2$  and identical, and after they are diagonalized we find (ignoring constants of order one)

$$m \sim s_{25} \left\{ 1 + \frac{1}{M_s^2} (s_{26} \cdot s_{15} + s_{26} \cdot s_{16}) + \frac{1}{M_s^4} (s_{26}^2 \cdot s_{15} \cdot s_{16} + s_{26}^2 \cdot s_{16}^2 + s_{26}^2 \cdot s_{15}^2) + \frac{1}{M_s^5} (s_4 \cdot s_6 \cdot s_9 \cdot s_{30} \cdot s_{18}) \left( \frac{s_{11} \pm s_5}{s_{25}} \right) \right\}. \quad (20)$$

It is clear that the following set of singlet VEVs is consistent with giving  $2 \times (\nu + \bar{\nu}) + 2 \times (y + \bar{y})$  a mass at  $M_{\text{EX}}$ :

$$\langle s_1 \rangle \sim \langle s_{25} \rangle \sim M_{\text{EX}}, \quad \text{all other singlets} \sim M_s. \quad (21)$$

Note that we do rely here on some suppression in the sixth-order term, so that it does not give an overwhelming [i.e.  $\mathcal{O}(M_s)$ ] contribution to the mass term. This may be viewed as an additional tuning in the singlet VEVs, on the order of 1 part in 10 or 20.

Finally we check whether the VEV assignment (21) is consistent with having some number of  $(1, 1)_{1,*} + (1, 1)_{-1,*}$  pairs with mass  $\sim M_{\text{EX}}$ . In general, the charged singlet mass matrix (if we ignore the possibility of intermediate scale mass for the  $\bar{f}^+ + f^-$ ) is  $14 \times 14$  with equally complicated eigenvalues, so we will omit the details of this analysis. Nevertheless, if we proceed in the same manner, we do find two linear combinations of singlets ( $s^+$  and  $s^-$ ) whose mass terms depend *explicitly* on the VEV  $\langle s_{25} \rangle$ , giving them naturally small mass terms.

We conclude that unification is possible *in principle* in model 1A. Specifically, in the absence of accidental cancellations, and assuming that higher-order terms in the superpotential are negligible (such that the light linear combination of the  $\delta$ 's remains light), we have found one version of model 1A that gives us gauge coupling unification. Namely, if we assume order one coefficients in the mass matrices, and that

$$\langle s_1 \rangle \sim \langle s_{25} \rangle \sim M_{\text{EX}}, \quad \text{all other singlets} \sim M_s, \quad (22)$$

we have exactly the following matter content in the theory with mass on the order of  $M_{\text{EX}}$ :

$$2 \times [\nu + \bar{\nu}] + 1 \times [y + \bar{y}] + 2 \times [s^+ + s^-] + [\delta + \bar{\delta}].$$

This corresponds to the solution marked with an arrow ( $\Rightarrow$ ) in Table VIII in Appendix C.<sup>11</sup> This gives us a prediction for the intermediate scale, the compactification scale, the string scale, and proton decay coming from

<sup>11</sup>Note that the states  $y$  are doublets under a hidden sector SU(2), so that  $1 \times [y + \bar{y}] \sim 2 \times [(1, \mathbf{2})_{0,*} + (1, \mathbf{2})_{0,*}]$ .

dimension six operators:

$$\begin{aligned} M_{\text{EX}} &\sim 1.9 \times 10^9 \text{ GeV}, & M_{\text{C}} &\sim 2.2 \times 10^{17} \text{ GeV}, \\ M_{\text{S}} &\sim 1.0 \times 10^{18} \text{ GeV}, & \tau(p \rightarrow e^+ \pi^0) &\sim 1.2 \times 10^{38} \text{ yr}. \end{aligned} \quad (23)$$

It is worth pointing out that this solution is not yet ruled out by the current bounds on proton decay, a fact which was not guaranteed. This model is pictured in the small red box in Fig. 5.

We note that the other option that one may try is, for example,

$$\begin{aligned} \langle s_{11} \rangle + \langle s_5 \rangle &\sim M_{\text{S}}, & \langle s_{11} \rangle - \langle s_5 \rangle &\sim M_{\text{EX}}, \\ \langle s_{25} \rangle &\sim \langle s_1 \rangle &\sim M_{\text{EX}}. \end{aligned} \quad (24)$$

This is a tuning to one part in  $M_{\text{S}}/M_{\text{EX}}$  and is consistent with  $F = 0$ , which is discussed below. This gives us one pair of  $v + \bar{v}$  and one  $y$ , and one pair of  $\delta + \bar{\delta}$  with exotic scale mass, assuming that we *cannot* neglect the sixth-order term in Eq. (20). The problem that one may encounter is with the charged singlets. Taking  $\langle s_{25} \rangle \sim M_{\text{EX}}$  generally gives one at least *two* charged singlets with mass at the intermediate scale, so one may need an additional tuning in that sector of the theory in order to realize one of the solutions in Table VIII.

$$F = 0$$

Let us now comment on the compatibility of these solutions with the constraint of  $F = 0$  in the case of model 1A. If we set all of the coefficients in the superpotential to one, the  $F$  flatness conditions can be solved exactly in this model. In units where  $M_{\text{S}} \equiv 1$ , we find the following relationships among the singlet VEVs:

$$s_{22} = -\frac{1}{s_{20} + s_{21}}(h_1 h_2 + s_{17} s_{18}) - s_{23}, \quad (25)$$

$$s_{26} = -\frac{1}{s_{15} + s_{16}}, \quad (26)$$

$$\begin{aligned} s_1 &= \frac{s_{15} + s_{16}}{s_{18}} \{h_1 h_{10} + h_2 h_9 + s_{17} s_{25} + s_{18} s_{27} \\ &\quad + (s_{15} + s_{16}) s_{30} + (s_{20} + s_{21}) s_{31}\}. \end{aligned} \quad (27)$$

The task is to now assign arbitrary VEVs to everything *except*  $s_{22}$ ,  $s_{26}$ , and  $s_1$  and look for solutions where  $s_1 \sim s_{25} \sim M_{\text{EX}}$ . The tuning in this model is evident in Eq. (27). It is clear that there must be a cancellation on the right-hand side of the equation to one part in  $M_{\text{S}}/M_{\text{EX}}$ . In general, one has no trouble finding numerical solutions to these equations such that  $s_1 \sim s_{25} \sim M_{\text{EX}}$ , while all other singlets have VEVs near the string scale.

One may object to the fact that we did not include superpotential coefficients in Eqs. (25)–(27), as it is clear that decoupling depends on these coefficients *not* being set to one. Solving the  $F$  flatness conditions with arbitrary superpotential coefficients is a computationally intensive problem. However, we expect that the inclusion of such coefficients will not significantly alter our conclusions.

## B. Model 2

The exotic matter content of model 2 is listed in Table IV. The brane-localized states which contribute to the differential running  $\alpha_3^{-1} - \alpha_2^{-1}$  are

$$\begin{aligned} v &\equiv (\mathbf{3}, 1)_{1/3, -4/3}, \\ m &\equiv (\mathbf{1}, \mathbf{2})_{0,*}, \quad \text{and} \quad y \equiv (\mathbf{1}, \mathbf{2})_{0,0}. \end{aligned} \quad (28)$$

In model 2 we have

$$\begin{aligned} 4 \times (v + \bar{v}) + 2 \times (y + \bar{y}) + 2 \times (m + \bar{m}) \\ + 20 \times (s^+ + s^-) + 2 \times (x^+ + x^-), \end{aligned} \quad (29)$$

where  $x^\pm$  are defined in Table IV.

The mass matrix for the  $v$  is a  $4 \times 4$  block diagonal matrix. The blocks are both  $2 \times 2$ , and the upper block turns out to be equivalent to the  $(2 \times 2)$  mass matrix for the  $y$ 's. By choosing

$$\langle h_2 \rangle \sim \langle s_{43} \rangle \sim M_{\text{EX}}, \quad \text{all other singlets} \sim M_{\text{S}}, \quad (30)$$

we find  $4 \times (v + \bar{v}) + 2 \times (y + \bar{y})$ . The problem with the VEV assignment in Eq. (30) is that we get too many charged singlets, so we will need to rely (heavily) on tuning arguments. Thus we conclude that, for model 2 to be consistent with gauge coupling unification, we must arrange a conspiracy among the singlet VEVs, such that we get intricate cancellations in the charged singlet sector.

## V. CONCLUSIONS

We have addressed the question of gauge coupling unification in a class of 15 mini-landscape models [40] with properties very similar to the MSSM. We analyze these  $E_8 \times E_8$  weakly coupled heterotic string models compactified on an anisotropic orbifold with one large ( $R$ ) and five small ( $l_s$ ) extra dimensions, where  $R \gg l_s$  and  $l_s$  is the string length. All of these theories can then be described in terms of an effective 5D  $SU(6)$  orbifold GUT field theory with compactification scale  $M_{\text{C}} = 1/R$  and cutoff scale  $M_{\text{S}} = 1/l_s$ .  $SU(6)$  is broken to the MSSM gauge group by orbifold boundary conditions at  $M_{\text{C}}$ , and gauge couplings must unify at the cutoff scale  $M_{\text{S}}$ . Moreover, in an orbifold GUT field theory, this is accomplished with the aid of Kaluza-Klein modes which contribute to the RG running above the compactification scale  $M_{\text{C}}$ .

In all 15 models the electroweak Higgs doublets reside in the (effective 4D,  $N = 2$ ) vector multiplet; hence, the models satisfy “gauge-Higgs unification.” In addition the third family of quarks and leptons are bulk modes, while the two lighter families are brane states. Although gauge-Higgs unification may be well motivated by aesthetics, we prove in Appendix A that gauge coupling unification is not possible if one includes only MSSM states and their KK towers. Thus it is necessary to also include the possible contribution of vectorlike exotics to the RG running. To simplify the analysis, we assume a small set of exotics obtain mass at a scale  $M_{\text{EX}} < M_C$  with the remainder obtaining mass at  $M_s$ . Using an effective field theory analysis, we find many solutions to gauge coupling unification labeled by the different inequivalent sets of exotics with mass at  $M_{\text{EX}}$ . These solutions are found in Tables VII, VIII, and IX in Appendix C.

We have analyzed two models in more detail (models 1A and 2 [40]), since for these models we have the superpotential up to order 6 in MSSM singlets. In this case, we have shown that one of our solutions (in model 1A) is consistent with string theory in a supersymmetric vacuum with  $F = 0$ , if we tune the singlet VEVs appropriately in Eq. (27). On the other hand, for the case of model 2, although there are many effective field theory solutions, we have not been able to demonstrate the existence of a simple string vacuum solution with  $F = 0$ . In this case, a solution may still be possible; however, it would require more fine-tuning.

Since quarks and leptons of the first two families are located on an effective SU(5) brane, they are subject to proton decay processes mediated by gauge exchange at the compactification scale  $M_C$ . Moreover, since  $M_C$  is generically less than the 4D GUT scale, the proton decay rate for the process  $p \rightarrow e^+ \pi^0$  is enhanced. Thus 80% of the models satisfying gauge coupling unification are excluded by Super-K bounds on proton decay. Most of the other models can be tested at a future proton decay detector.

All of the mini-landscape models have an exact  $R$  parity, so they do not suffer from dimension three or four baryon and/or lepton number violating processes. Moreover, the lightest supersymmetric particle is stable and a possible dark matter candidate. However, unlike 5D or 6D orbifold GUT field theories studied in the literature, these models suffer from uncontrolled dimension five operator contributions to proton decay. In particular, some of the vectorlike exotics have quantum numbers of color triplet Higgs multiplets. When given mass at  $M_s$  or  $M_{\text{EX}}$  they induce dimension five proton decay operators. Although it may be possible to fine-tune the coefficients of these operators to be small, it would be preferable to have a symmetry argument. This problem needs to be addressed in any future string model building.

As noted, all of the models studied in this analysis have a 5D (or 6D) SU(6) orbifold GUT limit. The complete

spectrum of the 6D model (prior to the final  $\mathbb{Z}_2$  orbifold and Wilson line  $A_2$ ) is given in Table III. It is very interesting to note that the spectrum is identical with the spectrum found in an  $E_8 \times E_8$  heterotic string compactified on a smooth  $K_3 \times T^2$  manifold with instantons embedded in the  $E_8 \times E_8$  gauge groups [62]. This suggests that these models may be obtained by the final  $\mathbb{Z}_2$  orbifolding of these smooth manifolds.

In conclusion, we have shown that gauge coupling unification may be accommodated in the present class of string models. However, a simple solution, without including vectorlike exotics below the string scale, was not possible. This appears to be a general conclusion stemming from the particular implementation of gauge-Higgs unification in these models. Finally, any future string model building needs to address the general problem of uncontrolled dimension five baryon and lepton number violating operators.

## ACKNOWLEDGMENTS

We would like to thank Gerry Cleaver, Hyun-Min Lee and Hasan Yüksel for illuminating conversations. This work is supported under DOE Grant No. DOE/ER/01545-878.

## APPENDIX A: COMPARING TWO SU(6) ORBIFOLD GUTS

The SU(6) orbifold GUTs considered in this paper satisfy the special property of gauge-Higgs unification. This is also a property of the 5D SU(6) orbifold GUT discussed in Ref. [42]. It is instructive to compare this SU(6) model to one without gauge-Higgs unification, in particular, the 5D SU(5) orbifold GUT discussed in Ref. [24].

In the models with gauge-Higgs unification, the Higgs multiplets come from the 5D *vector* multiplet ( $V, \Phi$ ), both in the adjoint representation of SU(6).  $V$  is the 4D gauge multiplet, and the 4D chiral multiplet  $\Phi$  contains the Higgs doublets. These states transform as follows under the orbifold parities ( $PP'$ ):

$$V: \begin{pmatrix} (++) & (++) & (++) & (+-) & (+-) & (-+) \\ (++) & (++) & (++) & (+-) & (+-) & (-+) \\ (++) & (++) & (++) & (+-) & (+-) & (-+) \\ (+-) & (+-) & (+-) & (++) & (++) & (--) \\ (+-) & (+-) & (+-) & (++) & (++) & (--) \\ (-+) & (-+) & (-+) & (--) & (--) & (++) \end{pmatrix}, \quad (\text{A1})$$

$$\Phi: \begin{pmatrix} (--) & (--) & (--) & (-+) & (-+) & (+-) \\ (--) & (--) & (--) & (-+) & (-+) & (+-) \\ (--) & (--) & (--) & (-+) & (-+) & (+-) \\ (-+) & (-+) & (-+) & (--) & (--) & (++) \\ (-+) & (-+) & (-+) & (--) & (--) & (++) \\ (+-) & (+-) & (+-) & (++) & (++) & (--) \end{pmatrix}. \quad (\text{A2})$$

Note the appearance of the MSSM Higgs multiplets in  $\Phi$  with  $(++)$  boundary conditions, and its partner in  $V$  with  $(--)$  boundary conditions. These massive KK states contribute to a logarithmic running of the gauge couplings with a term of the form

$$\alpha_i^{-1} \supset -\frac{1}{4\pi}(b_i^{++} + b_i^{--}) \log \frac{M_s}{M_c}. \quad (\text{A3})$$

We find for the model of Ref. [42] (including just  $V$ ,  $\Phi$  above)

$$\vec{b}^{++} = (-9, -5, 3/5), \quad \vec{b}^{--} = (3, -1, -9/5),$$

$$\vec{b}^{++} + \vec{b}^{--} = (-6, -6, -6/5). \quad (\text{A4})$$

(These numbers can be calculated using the values in Table VI.) Again we stress that the only difference between the models presented in this paper and that of Ref. [42] is that the third family lives in the bulk in our constructions, which will change these numbers by only a universal contribution. Indeed, one can check by comparing Eq. (A4) with (9) that the only difference is a family universal contribution.

This can then be compared to an  $SU(5)$  model without gauge-Higgs unification [24]. In this case the 5D gauge multiplet includes the states, with their transformation under the orbifold parities ( $PP'$ ):

$$V: \begin{pmatrix} (++) & (++) & (++) & (+-) & (+-) \\ (++) & (++) & (++) & (+-) & (+-) \\ (++) & (++) & (++) & (+-) & (+-) \\ (+-) & (+-) & (+-) & (++) & (++) \\ (+-) & (+-) & (+-) & (++) & (++) \end{pmatrix}, \quad (\text{A5})$$

$$\Phi: \begin{pmatrix} (--) & (--) & (--) & (-+) & (-+) \\ (--) & (--) & (--) & (-+) & (-+) \\ (--) & (--) & (--) & (-+) & (-+) \\ (-+) & (-+) & (-+) & (--) & (--) \\ (-+) & (-+) & (-+) & (--) & (--) \end{pmatrix}. \quad (\text{A6})$$

The Higgs multiplets are contained in the chiral multiplets  $H_5 + H_5^c$  and  $H_{\bar{5}} + H_{\bar{5}}^c$ , with parities

$$H_5, H_{\bar{5}}: \begin{pmatrix} (+-) \\ (+-) \\ (+-) \\ (++) \\ (++) \end{pmatrix}, \quad (\text{A7})$$

$$H_5^c, H_{\bar{5}}^c: \begin{pmatrix} (-+) \\ (-+) \\ (-+) \\ (--) \\ (--) \end{pmatrix}. \quad (\text{A8})$$

In this case, the  $(--)$  partners of the Higgs doublets

appear in chiral multiplets *not the gauge multiplet* as before. Thus we now find the beta function coefficients given by

$$\vec{b}^{++} = (-9, -5, 3/5), \quad \vec{b}^{--} = (3, 3, 3/5),$$

$$\vec{b}^{++} + \vec{b}^{--} = (-6, -2, 6/5). \quad (\text{A9})$$

To get relationships between the cutoff ( $M_s$ ) and the compactification scale ( $M_c$ ), we can compare  $5\alpha_1^{-1}(M_c) - 3\alpha_2^{-1}(M_c) - 2\alpha_3^{-1}(M_c)$  and  $\alpha_3^{-1}(M_c f) - \alpha_2^{-1}(M_c)$  in the orbifold GUT and in the MSSM. Including the threshold correction in Eq. (3) we find (for gauge-Higgs unification)

$$\log \frac{M_{\text{GUT}}}{M_c} = \frac{2}{3} \log \frac{M_s}{M_c} + \frac{1}{3}, \quad \log \frac{M_s}{M_{\text{GUT}}} = -\frac{3}{2}. \quad (\text{A10})$$

The factors of  $\frac{1}{3}$  and  $-\frac{3}{2}$  come from the threshold correction applied at  $M_{\text{GUT}}$ . These equations implicitly assume the relation  $M_c \leq M_{\text{GUT}}, M_s$ ; however, the solution to the equation gives the unphysical relation  $M_c > M_{\text{GUT}} > M_s$ . This is the main reason we need to rely on light exotics. On the other hand, for the  $SU(5)$  orbifold GUT we find

$$\log \frac{M_{\text{GUT}}}{M_c} = \frac{2}{3} \log \frac{M_s}{M_c} + \frac{1}{3}, \quad \log \frac{M_{\text{GUT}}}{M_c} = \frac{1}{2} \log \frac{M_s}{M_c} + \frac{3}{2}, \quad (\text{A11})$$

which gives the physically acceptable solution  $\log \frac{M_s}{M_{\text{GUT}}} = 2$  and  $\log \frac{M_{\text{GUT}}}{M_c} = 5$ . We thus conclude that simple gauge-Higgs unification in 5D  $SU(6)$  is not viable.

In Ref. [42] an  $N = 2$  model with gauge-Higgs unification in 6D (or  $N = 4$  in 4D) was also considered. In this case the Higgs multiplet and its  $(--)$  partners are contained in chiral adjoints. Gauge coupling unification works in this model. Unfortunately, we do not know how to obtain such a model from the heterotic string.

Of course, the additional problem concerning gauge coupling unification in the context of the heterotic string is the need to match the low-energy values of the coupling constants given values of  $M_c$  and  $M_s$ . In particular, we must satisfy the relation

$$\alpha_{\text{STRING}}^{-1} = \frac{1}{8} \left( \frac{M_{\text{PL}}}{M_s} \right)^2. \quad (\text{A12})$$

In most cases, with  $M_c \leq M_{\text{GUT}} < M_s$ , the power-law running due to the KK modes is required, i.e.

$$\alpha_i^{-1}(M_c) \supset \alpha_{\text{STRING}}^{-1} + \frac{b_i^G}{2\pi} \left( \frac{M_s}{M_c} - 1 \right) + \text{long terms}$$

$$\sim \mathcal{O}(10). \quad (\text{A13})$$



## APPENDIX B: CONSTRAINTS FROM PROTON DECAY

### 1. Dimension six operators

The gauge bosons in GUTs can mediate proton decay via effective dimension six operators. The best bounds on proton decay come from the channel  $p \rightarrow e^+ + \pi^0$ , and current (published) experimental limits are [31]

$$\tau(p \rightarrow e^+ + \pi^0) > 1.6 \times 10^{33} \text{ yr.} \quad (\text{B1})$$

In this paper, we are looking at an SU(6) GUT in five dimensions, which is broken to either SU(5) or SU(4)  $\times$  SU(2) on the branes. The dangerous operators come from SU(5) gauge boson (**X**) exchange and have been calculated in Ref. [63]. In a 4D SU(5) GUT, the effective Lagrangian leading to proton decay from **X** boson exchange is given by

$$\mathcal{L}_{\text{eff}} = \frac{g_{\text{GUT}}^2}{2M_{\text{X}}^2} J^\mu J_\mu^*, \quad (\text{B2})$$

where

$$J^\mu = -(l^*)^\mu \bar{\sigma}^\mu d^c + (u^c)^* \bar{\sigma}^\mu q + (q)^* \bar{\sigma}^\mu e^c + \text{H.c.} \quad (\text{B3})$$

The operators which lead to proton decay are given by

$$\begin{aligned} \mathcal{L}_{\text{eff}} = & -\frac{g_{\text{GUT}}^2}{2M_{\text{X}}^2} \sum_{i,j} [(q_i^* \bar{\sigma}^\mu u_i^c)(\ell^* \bar{\sigma}_\mu d_j^c) \\ & + (q_i^* \bar{\sigma}^\mu e_i^c)(q_j^* \bar{\sigma}_\mu u_j^c)]. \end{aligned} \quad (\text{B4})$$

The decay rate of  $p \rightarrow \pi^0 e^+$  in the 4D theory is given by

$$\begin{aligned} \Gamma(p \rightarrow \pi^0 e^+) = & \frac{(m_p^2 - m_\pi^2)^2}{64\pi m_p^3 f_\pi^2} \beta_{\text{LAT}}^2 A^2 \frac{g_{\text{GUT}}^4}{M_{\text{X}}^4} (1 + D + F)^2 \\ & \times [(1 + |V_{ud}|^2)^2 + 1]. \end{aligned} \quad (\text{B5})$$

These formulas will receive modifications in our model, based on the fact that there is a relationship among the string scale, the Planck scale and the coupling constant [see Eq. (2)] and that the whole tower of KK modes associated with the SU(5) gauge bosons will contribute to the decay rate.

Explicitly, the decay rate goes like  $g_{\text{GUT}}^4$ . We replace this by

$$g_{\text{GUT}}^4 \rightarrow (4\pi)^2 \alpha_{\text{STRING}}^2 = 64 \times (4\pi)^2 \times \left(\frac{M_s}{M_{\text{PL}}}\right)^4. \quad (\text{B6})$$

Next, we should consider the relationship between the compactification scale and the **X** boson mass. The SU(5) gauge bosons have  $(+ -)$  boundary conditions and masses of  $m_n = (n + \frac{1}{2})M_c$ . Proton decay can proceed by exchange of any of the tower of KK modes, which suggests we take

$$\frac{1}{M_{\text{X}}^2} \rightarrow 2 \times \frac{1}{M_c^2} \sum_{n=0}^{\infty} \frac{1}{(n + \frac{1}{2})^2} = \frac{\pi^2}{M_c^2}. \quad (\text{B7})$$

The factor of 2 comes from the fact that the KK modes of the gauge bosons are normalized differently than the zero modes [24].<sup>12</sup> Including all corrections, we make the replacement

$$\frac{g_{\text{GUT}}^4}{M_{\text{X}}^4} \rightarrow 64 \times (4\pi)^2 \times \left(\frac{M_s}{M_{\text{PL}}}\right)^4 \times \frac{\pi^4}{M_c^4}. \quad (\text{B8})$$

In our 5D orbifold GUT, we find

$$\Gamma(p \rightarrow \pi^0 e^+) \cong 4.00 \times 10^{-73} \left(\frac{M_s}{M_c}\right)^4 \text{ GeV}, \quad (\text{B9})$$

where we have used  $A = 3.4$ ,  $D = 0.80$  and  $F = 0.44$ , and  $\beta_{\text{LAT}} \cong 0.011 \text{ GeV}^3$  [41]. For the proton lifetime, we find

$$\tau(p \rightarrow \pi^0 e^+) \cong 5.21 \times 10^{40} \left(\frac{M_c}{M_s}\right)^4 \text{ yr.} \quad (\text{B10})$$

This corresponds to an upper limit on the ratio between the string scale and the compactification scale of

$$\frac{M_s}{M_c} \lesssim 75. \quad (\text{B11})$$

Alternatively, given a (typical) string scale of about  $5 \times 10^{17} \text{ GeV}$ , this corresponds to

$$M_c \gtrsim 6.6 \times 10^{15} \text{ GeV.} \quad (\text{B12})$$

An interesting difference between this result and the result one typically finds in an orbifold GUT (see, for example, Ref. [64]) is that the proton lifetime no longer scales like the compactification scale directly but as a ratio of scales. This means that the compactification scale can be smaller than  $M_c \sim 6.6 \times 10^{15} \text{ GeV}$  if the string scale is sufficiently small, which means that the underlying GUT is very weakly coupled ( $\alpha_{\text{GUT}} \ll 1$ ).<sup>13</sup> We note that this is an additional constraint that has no analogy in typical orbifold GUT model building, imposed by the relationship among the coupling constant, Newton's constant, and  $\alpha'$ . Finally, in the interesting limit that  $M_c \rightarrow M_s$ , we find the upper bound on the proton lifetime in this class of models:  $\tau(p \rightarrow \pi^0 e^+) \lesssim 5.21 \times 10^{40} \text{ yr.}$

<sup>12</sup>Equivalently, one can understand this factor as the Kaluza-Klein tower of gauge bosons coupling *more strongly* to the fermions by a factor of  $\sqrt{2}$ , which corresponds to rescaling  $g_{\text{GUT}} \rightarrow \sqrt{2} g_{\text{GUT}}$ .

<sup>13</sup>This may correspond to a region where the string coupling constant  $g_{\text{STRING}} \sim e^\phi$  (where  $\phi$  is the dilaton field) is no longer small. This is undesirable, as we wish to embed these models in the weakly coupled heterotic string [65].

## 2. Dimension five operators

In supersymmetric theories, the proton may decay via dimension five operators as well. In the mini-landscape models [40], the  $(\mathbf{3}, 1)_{-2/3, -2/3} + (\bar{\mathbf{3}}, 1)_{2/3, 2/3}$  states, called  $\delta$  and  $\bar{\delta}$ , can mediate proton decay via dimension five operators—they have the same gauge quantum numbers as color triplet Higgses. It was shown in Ref. [7] that the effective mass of the color triplet Higgsino  $M_{\tilde{H}} \sim 10^{18} - 10^{21}$  GeV has to be much larger than the (four-dimensional) GUT scale in order to evade bounds on  $p \rightarrow K^+ \bar{\nu}$ , depending on the soft SUSY breaking parameters.

The  $\delta$  particles have the same quantum numbers as color triplet Higgses, and thus we expect similar bounds for them

(assuming they couple to quarks and leptons with small effective Yukawa couplings). Unfortunately, to make matters worse, it was found in Ref. [40] that the  $\delta$  states have tree level coupling to the quarks in the superpotential, and so the coupling is naturally of order one, i.e. *not* suppressed by Yukawa factors as they are in the typical dimension five proton decay operator. However, by carefully adjusting the singlet VEVs that describe the  $\delta$ ,  $\bar{\delta}$  interactions, this problem can be avoided, but currently we are lacking a mechanism that would naturally suppress this decay channel for the proton.

## APPENDIX C: MISCELLANY

TABLE I. Spectrum of model 1 of the mini-landscape search [40]. From the viewpoint of the five-dimensional theory, all states that are not localized in the SO(4) torus ( $U$ ,  $T_2$ ,  $T_4$ ) are bulk modes. The symbols  $\bullet$ ,  $\star$ ,  $\blacksquare$ , and  $\blacktriangle$  indicate the localization of the brane modes in the SO(4) torus; compare Fig. 2.

$U$		$T_3$		$T_5$			
$1 \times (\mathbf{3}, \mathbf{2})_{1/3, 1/3}$	Bulk	$4 \times (\mathbf{1}, \mathbf{1})_{1, 3}$	$\blacktriangle$	$1 \times (\mathbf{3}, \mathbf{2})_{1/3, 1/3}$	$\star$	$1 \times (\mathbf{1}, \mathbf{1})_{-1, -3}$	$\blacksquare$
$1 \times (\bar{\mathbf{3}}, \mathbf{1})_{-4/3, -1/3}$	Bulk	$4 \times (\mathbf{1}, \mathbf{1})_{-1, -3}$	$\blacktriangle$	$1 \times (\mathbf{3}, \mathbf{2})_{1/3, 1/3}$	$\bullet$	$1 \times (\mathbf{1}, \mathbf{1})_{1, -3}$	$\blacktriangle$
$1 \times (\mathbf{1}, \mathbf{2})_{1, 0}$	Bulk	$4 \times (\mathbf{1}, \mathbf{1})_{1, 3}$	$\blacksquare$	$1 \times (\bar{\mathbf{3}}, \mathbf{1})_{-4/3, -1/3}$	$\star$	$1 \times (\mathbf{1}, \mathbf{1})_{1, 3}$	$\blacktriangle$
$1 \times (\mathbf{1}, \mathbf{2})_{-1, 0}$	Bulk	$4 \times (\mathbf{1}, \mathbf{1})_{-1, -3}$	$\blacksquare$	$1 \times (\bar{\mathbf{3}}, \mathbf{1})_{-4/3, -1/3}$	$\bullet$	$1 \times (\mathbf{1}, \mathbf{1})_{1, 3}$	$\blacksquare$
$1 \times (\mathbf{1}, \mathbf{1})_{2, 1}$	Bulk	$2 \times (\mathbf{1}, \mathbf{1})_{1, 2}$	$\blacktriangle$	$1 \times (\bar{\mathbf{3}}, \mathbf{1})_{2/3, -1/3}$	$\star$	$1 \times (\mathbf{1}, \mathbf{1})_{1, -3}$	$\blacksquare$
$4 \times (\mathbf{1}, \mathbf{1})_{0, -1}$	Bulk	$2 \times (\mathbf{1}, \mathbf{1})_{-1, -2}$	$\blacktriangle$	$1 \times (\bar{\mathbf{3}}, \mathbf{1})_{2/3, -1/3}$	$\bullet$	$2 \times (\mathbf{1}, \mathbf{1})_{1, -2}$	$\blacktriangle$
$5 \times (\mathbf{1}, \mathbf{1})_{0, 1}$	Bulk	$2 \times (\mathbf{1}, \mathbf{1})_{1, 2}$	$\blacksquare$	$1 \times (\bar{\mathbf{3}}, \mathbf{1})_{-1/3, 8/3}$	$\blacktriangle$	$2 \times (\mathbf{1}, \mathbf{1})_{-1, 2}$	$\blacktriangle$
$2 \times (\mathbf{1}, \mathbf{1})_{0, 0}$	Bulk	$2 \times (\mathbf{1}, \mathbf{1})_{-1, -2}$	$\blacksquare$	$1 \times (\mathbf{3}, \mathbf{1})_{1/3, -8/3}$	$\blacktriangle$	$2 \times (\mathbf{1}, \mathbf{1})_{1, -2}$	$\blacksquare$
$T_2$		$1 \times (\mathbf{1}, \mathbf{1})_{1, 2}$	$\blacktriangle$	$1 \times (\bar{\mathbf{3}}, \mathbf{1})_{-1/3, 8/3}$	$\blacksquare$	$2 \times (\mathbf{1}, \mathbf{1})_{-1, 2}$	$\blacksquare$
$3 \times (\bar{\mathbf{3}}, \mathbf{1})_{2/3, 2/3}$	Bulk	$1 \times (\mathbf{1}, \mathbf{1})_{1, -2}$	$\blacktriangle$	$1 \times (\mathbf{3}, \mathbf{1})_{1/3, -8/3}$	$\blacksquare$	$1 \times (\mathbf{1}, \mathbf{1})_{0, 5}$	$\star$
$3 \times (\mathbf{3}, \mathbf{1})_{-2/3, -2/3}$	Bulk	$1 \times (\mathbf{1}, \mathbf{1})_{1, -2}$	$\blacksquare$	$1 \times (\mathbf{1}, \mathbf{2})_{-1, -1}$	$\star$	$1 \times (\mathbf{1}, \mathbf{1})_{0, -5}$	$\star$
$2 \times (\bar{\mathbf{3}}, \mathbf{1})_{2/3, -1/3}$	Bulk	$1 \times (\mathbf{1}, \mathbf{1})_{-1, 2}$	$\blacksquare$	$1 \times (\mathbf{1}, \mathbf{2})_{-1, -1}$	$\bullet$	$1 \times (\mathbf{1}, \mathbf{1})_{0, 5}$	$\bullet$
$1 \times (\mathbf{1}, \mathbf{2})_{1, 1}$	Bulk	$1 \times (\mathbf{1}, \mathbf{1})_{0, 6}$	$\star$	$1 \times (\mathbf{1}, \mathbf{2})_{0, -3}$	$\blacktriangle$	$1 \times (\mathbf{1}, \mathbf{1})_{0, -5}$	$\bullet$
$3 \times (\mathbf{1}, \mathbf{1})_{0, 5}$	Bulk	$1 \times (\mathbf{1}, \mathbf{1})_{0, -6}$	$\star$	$1 \times (\mathbf{1}, \mathbf{2})_{0, 3}$	$\blacktriangle$	$2 \times (\mathbf{1}, \mathbf{1})_{0, 3}$	$\star$
$6 \times (\mathbf{1}, \mathbf{1})_{0, 3}$	Bulk	$1 \times (\mathbf{1}, \mathbf{1})_{0, 6}$	$\bullet$	$1 \times (\mathbf{1}, \mathbf{2})_{0, 3}$	$\blacksquare$	$2 \times (\mathbf{1}, \mathbf{1})_{0, -3}$	$\star$
$4 \times (\mathbf{1}, \mathbf{1})_{0, 2}$	Bulk	$1 \times (\mathbf{1}, \mathbf{1})_{0, -6}$	$\bullet$	$1 \times (\mathbf{1}, \mathbf{2})_{0, -3}$	$\blacksquare$	$2 \times (\mathbf{1}, \mathbf{1})_{0, 3}$	$\bullet$
$4 \times (\mathbf{1}, \mathbf{1})_{0, -2}$	Bulk	$2 \times (\mathbf{1}, \mathbf{1})_{0, -2}$	$\star$	$1 \times (\mathbf{1}, \mathbf{2})_{0, 2}$	$\blacktriangle$	$2 \times (\mathbf{1}, \mathbf{1})_{0, -3}$	$\bullet$
$5 \times (\mathbf{1}, \mathbf{1})_{0, 1}$	Bulk	$2 \times (\mathbf{1}, \mathbf{1})_{0, 2}$	$\star$	$1 \times (\mathbf{1}, \mathbf{2})_{0, -2}$	$\blacktriangle$	$1 \times (\mathbf{1}, \mathbf{1})_{0, -1}$	$\star$
$2 \times (\mathbf{1}, \mathbf{1})_{0, -1}$	Bulk	$2 \times (\mathbf{1}, \mathbf{1})_{0, -2}$	$\bullet$	$1 \times (\mathbf{1}, \mathbf{2})_{0, 2}$	$\blacksquare$	$1 \times (\mathbf{1}, \mathbf{1})_{0, -1}$	$\bullet$
$21 \times (\mathbf{1}, \mathbf{1})_{0, 0}$	Bulk	$2 \times (\mathbf{1}, \mathbf{1})_{0, 2}$	$\bullet$	$1 \times (\mathbf{1}, \mathbf{2})_{0, -2}$	$\blacksquare$	$1 \times (\mathbf{1}, \mathbf{1})_{0, 1}$	$\star$
$T_4$				$2 \times (\mathbf{1}, \mathbf{2})_{0, 0}$	$\blacktriangle$	$1 \times (\mathbf{1}, \mathbf{1})_{0, 1}$	$\star$
$3 \times (\bar{\mathbf{3}}, \mathbf{1})_{2/3, 2/3}$	Bulk			$2 \times (\mathbf{1}, \mathbf{2})_{0, 0}$	$\blacksquare$	$1 \times (\mathbf{1}, \mathbf{1})_{0, 1}$	$\bullet$
$3 \times (\mathbf{3}, \mathbf{1})_{-2/3, -2/3}$	Bulk			$1 \times (\mathbf{1}, \mathbf{1})_{2, 1}$	$\star$	$1 \times (\mathbf{1}, \mathbf{1})_{0, 1}$	$\bullet$
$1 \times (\bar{\mathbf{3}}, \mathbf{1})_{-2/3, 1/3}$	Bulk			$1 \times (\mathbf{1}, \mathbf{1})_{2, 1}$	$\bullet$	$8 \times (\mathbf{1}, \mathbf{1})_{0, 0}$	$\star$
$2 \times (\mathbf{1}, \mathbf{2})_{-1, -1}$	Bulk			$1 \times (\mathbf{1}, \mathbf{1})_{-1, -3}$	$\blacktriangle$	$8 \times (\mathbf{1}, \mathbf{1})_{0, 0}$	$\star$
$3 \times (\mathbf{1}, \mathbf{1})_{0, -5}$	Bulk			$1 \times (\mathbf{1}, \mathbf{1})_{-1, 3}$	$\blacktriangle$	$6 \times (\mathbf{1}, \mathbf{1})_{0, 0}$	$\bullet$
$6 \times (\mathbf{1}, \mathbf{1})_{0, -3}$	Bulk			$1 \times (\mathbf{1}, \mathbf{1})_{-1, 3}$	$\blacksquare$	$6 \times (\mathbf{1}, \mathbf{1})_{0, 0}$	$\bullet$
$2 \times (\mathbf{1}, \mathbf{1})_{0, -2}$	Bulk						
$2 \times (\mathbf{1}, \mathbf{1})_{0, 2}$	Bulk						
$1 \times (\mathbf{1}, \mathbf{1})_{0, 1}$	Bulk						
$4 \times (\mathbf{1}, \mathbf{1})_{0, -1}$	Bulk						
$21 \times (\mathbf{1}, \mathbf{1})_{0, 0}$	Bulk						

TABLE II. Spectrum of model 2 of the mini-landscape search [40]. From the viewpoint of the five-dimensional theory, all states that are not localized in the  $SO(4)$  torus ( $U$ ,  $T_2$ ,  $T_4$ ) are bulk modes. The symbols  $\bullet$ ,  $\star$ ,  $\blacksquare$ , and  $\blacktriangle$  indicate the localization of the brane modes in the  $SO(4)$  torus; compare Fig. 2.

$U$		$T_3$		$T_5$			
$1 \times (\mathbf{3}, \mathbf{2})_{1/3, 1/3}$	Bulk	$1 \times (\mathbf{3}, \mathbf{1})_{1/3, -8/3}$	$\blacktriangle$	$1 \times (\mathbf{3}, \mathbf{2})_{1/3, 1/3}$	$\star$	$2 \times (\mathbf{1}, \mathbf{1})_{-1, -2}$	$\blacksquare$
$1 \times (\bar{\mathbf{3}}, \mathbf{1})_{-4/3, -1/3}$	Bulk	$1 \times (\bar{\mathbf{3}}, \mathbf{1})_{-1/3, 8/3}$	$\blacktriangle$	$1 \times (\mathbf{3}, \mathbf{2})_{1/3, 1/3}$	$\bullet$	$2 \times (\mathbf{1}, \mathbf{1})_{1, 1}$	$\blacktriangle$
$1 \times (\mathbf{1}, \mathbf{2})_{1, 0}$	Bulk	$1 \times (\mathbf{3}, \mathbf{1})_{1/3, -8/3}$	$\blacksquare$	$1 \times (\bar{\mathbf{3}}, \mathbf{1})_{-4/3, -1/3}$	$\star$	$2 \times (\mathbf{1}, \mathbf{1})_{1, -1}$	$\blacktriangle$
$1 \times (\mathbf{1}, \mathbf{2})_{-1, 0}$	Bulk	$1 \times (\bar{\mathbf{3}}, \mathbf{1})_{-1/3, 8/3}$	$\blacksquare$	$1 \times (\bar{\mathbf{3}}, \mathbf{1})_{-4/3, -1/3}$	$\bullet$	$2 \times (\mathbf{1}, \mathbf{1})_{-1, 1}$	$\blacktriangle$
$1 \times (\mathbf{1}, \mathbf{1})_{2, 1}$	Bulk	$3 \times (\mathbf{1}, \mathbf{1})_{1, 3}$	$\blacktriangle$	$1 \times (\bar{\mathbf{3}}, \mathbf{1})_{2/3, -1/3}$	$\star$	$2 \times (\mathbf{1}, \mathbf{1})_{-1, -1}$	$\blacktriangle$
$1 \times (\mathbf{1}, \mathbf{1})_{0, -2}$	Bulk	$3 \times (\mathbf{1}, \mathbf{1})_{-1, -3}$	$\blacktriangle$	$1 \times (\bar{\mathbf{3}}, \mathbf{1})_{2/3, -1/3}$	$\bullet$	$2 \times (\mathbf{1}, \mathbf{1})_{1, -1}$	$\blacksquare$
$1 \times (\mathbf{1}, \mathbf{1})_{0, 2}$	Bulk	$3 \times (\mathbf{1}, \mathbf{1})_{1, 3}$	$\blacksquare$	$1 \times (\bar{\mathbf{3}}, \mathbf{1})_{-1/3, 5/3}$	$\blacktriangle$	$2 \times (\mathbf{1}, \mathbf{1})_{1, 1}$	$\blacksquare$
$8 \times (\mathbf{1}, \mathbf{1})_{0, 1/2}$	Bulk	$3 \times (\mathbf{1}, \mathbf{1})_{-1, -3}$	$\blacksquare$	$1 \times (\mathbf{3}, \mathbf{1})_{1/3, -5/3}$	$\blacktriangle$	$2 \times (\mathbf{1}, \mathbf{1})_{-1, 1}$	$\blacksquare$
$1 \times (\mathbf{1}, \mathbf{1})_{0, 0}$	Bulk	$1 \times (\mathbf{1}, \mathbf{1})_{1, -2}$	$\blacktriangle$	$1 \times (\bar{\mathbf{3}}, \mathbf{1})_{-1/3, 5/3}$	$\blacksquare$	$2 \times (\mathbf{1}, \mathbf{1})_{-1, -1}$	$\blacksquare$
$T_2$		$1 \times (\mathbf{1}, \mathbf{1})_{-1, 2}$	$\blacktriangle$	$1 \times (\mathbf{3}, \mathbf{1})_{1/3, -5/3}$	$\blacksquare$	$1 \times (\mathbf{1}, \mathbf{1})_{1, 0}$	$\blacktriangle$
$3 \times (\mathbf{3}, \mathbf{1})_{-2/3, -2/3}$	Bulk	$1 \times (\mathbf{1}, \mathbf{1})_{1, -2}$	$\blacksquare$	$1 \times (\mathbf{1}, \mathbf{2})_{-1, -1}$	$\star$	$1 \times (\mathbf{1}, \mathbf{1})_{-1, 0}$	$\blacktriangle$
$1 \times (\mathbf{3}, \mathbf{1})_{-2/3, 1/3}$	Bulk	$1 \times (\mathbf{1}, \mathbf{1})_{-1, 2}$	$\blacksquare$	$1 \times (\mathbf{1}, \mathbf{2})_{-1, -1}$	$\bullet$	$1 \times (\mathbf{1}, \mathbf{1})_{1, 0}$	$\blacksquare$
$2 \times (\mathbf{1}, \mathbf{2})_{-1, -1}$	Bulk	$1 \times (\mathbf{1}, \mathbf{1})_{0, 3}$	$\star$	$1 \times (\mathbf{1}, \mathbf{2})_{0, -1}$	$\blacktriangle$	$1 \times (\mathbf{1}, \mathbf{1})_{-1, 0}$	$\blacksquare$
$3 \times (\mathbf{1}, \mathbf{2})_{-1, 0}$	Bulk	$1 \times (\mathbf{1}, \mathbf{1})_{0, -3}$	$\star$	$1 \times (\mathbf{1}, \mathbf{2})_{0, 1}$	$\blacktriangle$	$1 \times (\mathbf{1}, \mathbf{1})_{0, 3}$	$\star$
$6 \times (\mathbf{1}, \mathbf{1})_{0, 2}$	Bulk	$1 \times (\mathbf{1}, \mathbf{1})_{0, 3}$	$\bullet$	$1 \times (\mathbf{1}, \mathbf{2})_{0, 1}$	$\blacksquare$	$1 \times (\mathbf{1}, \mathbf{1})_{0, -3}$	$\star$
$6 \times (\mathbf{1}, \mathbf{1})_{0, -2}$	Bulk	$1 \times (\mathbf{1}, \mathbf{1})_{0, -3}$	$\bullet$	$1 \times (\mathbf{1}, \mathbf{2})_{0, -1}$	$\blacksquare$	$1 \times (\mathbf{1}, \mathbf{1})_{0, -3}$	$\bullet$
$6 \times (\mathbf{1}, \mathbf{1})_{0, -1}$	Bulk	$2 \times (\mathbf{1}, \mathbf{1})_{0, -2}$	$\star$	$2 \times (\mathbf{1}, \mathbf{2})_{0, 0}$	$\blacktriangle$	$1 \times (\mathbf{1}, \mathbf{1})_{0, 3}$	$\bullet$
$5 \times (\mathbf{1}, \mathbf{1})_{0, 1}$	Bulk	$2 \times (\mathbf{1}, \mathbf{1})_{0, 2}$	$\star$	$2 \times (\mathbf{1}, \mathbf{2})_{0, 0}$	$\blacksquare$	$2 \times (\mathbf{1}, \mathbf{1})_{0, -2}$	$\star$
$16 \times (\mathbf{1}, \mathbf{1})_{0, -1/2}$	Bulk	$2 \times (\mathbf{1}, \mathbf{1})_{0, -2}$	$\bullet$	$1 \times (\mathbf{1}, \mathbf{1})_{2, 1}$	$\star$	$2 \times (\mathbf{1}, \mathbf{1})_{0, 2}$	$\star$
$21 \times (\mathbf{1}, \mathbf{1})_{0, 0}$	Bulk	$2 \times (\mathbf{1}, \mathbf{1})_{0, 2}$	$\bullet$	$1 \times (\mathbf{1}, \mathbf{1})_{2, 1}$	$\bullet$	$2 \times (\mathbf{1}, \mathbf{1})_{0, 2}$	$\bullet$
$T_4$				$1 \times (\mathbf{1}, \mathbf{1})_{1, -2}$	$\blacktriangle$	$2 \times (\mathbf{1}, \mathbf{1})_{0, -2}$	$\bullet$
$3 \times (\bar{\mathbf{3}}, \mathbf{1})_{2/3, 2/3}$	Bulk			$2 \times (\mathbf{1}, \mathbf{1})_{1, 2}$	$\blacktriangle$	$3 \times (\mathbf{1}, \mathbf{1})_{0, 1}$	$\star$
$2 \times (\bar{\mathbf{3}}, \mathbf{1})_{2/3, -1/3}$	Bulk			$2 \times (\mathbf{1}, \mathbf{1})_{-1, -2}$	$\blacktriangle$	$2 \times (\mathbf{1}, \mathbf{1})_{0, -1}$	$\star$
$1 \times (\mathbf{1}, \mathbf{2})_{1, 1}$	Bulk			$1 \times (\mathbf{1}, \mathbf{1})_{-1, 2}$	$\blacktriangle$	$2 \times (\mathbf{1}, \mathbf{1})_{0, -1}$	$\bullet$
$3 \times (\mathbf{1}, \mathbf{2})_{1, 0}$	Bulk			$2 \times (\mathbf{1}, \mathbf{1})_{1, 2}$	$\blacksquare$	$3 \times (\mathbf{1}, \mathbf{1})_{0, 1}$	$\bullet$
$6 \times (\mathbf{1}, \mathbf{1})_{0, 2}$	Bulk			$1 \times (\mathbf{1}, \mathbf{1})_{1, -2}$	$\blacksquare$	$12 \times (\mathbf{1}, \mathbf{1})_{0, 0}$	$\star$
$6 \times (\mathbf{1}, \mathbf{1})_{0, -2}$	Bulk			$1 \times (\mathbf{1}, \mathbf{1})_{-1, 2}$	$\blacksquare$	$12 \times (\mathbf{1}, \mathbf{1})_{0, 0}$	$\bullet$
$4 \times (\mathbf{1}, \mathbf{1})_{0, -1}$	Bulk						
$6 \times (\mathbf{1}, \mathbf{1})_{0, 1}$	Bulk						
$8 \times (\mathbf{1}, \mathbf{1})_{0, 1/2}$	Bulk						
$12 \times (\mathbf{1}, \mathbf{1})_{0, 0}$	Bulk						

TABLE III. The full (five-dimensional) spectrum of the models that we analyze [39]. Note that  $\mathbf{8}_{v+c+s} \equiv \mathbf{8}_v + \mathbf{8}_c + \mathbf{8}_s$ . In five dimensions, both models 1 and 2 have the gauge group  $SU(6) \times [SO(8) \times SU(3)]'$ . Note that states are written in the language of  $D = 5$ ,  $N = 1$ , and that the spectrum of these models are identical to those examined by Ref. [61].

Multiplet type	Representation	Number
Tensor	Singlet	1
Vector	$(\mathbf{35}, 1, 1) \oplus (1, \mathbf{28}, 1)$	35 + 28
	$\oplus (1, 1, \mathbf{8}) \oplus 5 \times (1, 1, 1)$	8 + 5
Hyper	$(\mathbf{20}, 1, 1) \oplus (1, \mathbf{8}_{v+c+s}, 1) \oplus 4 \times (1, 1, 1)$	20 + 24 + 4
	$\oplus 9 \times \{(\mathbf{6}, 1, 1) \oplus (\bar{\mathbf{6}}, 1, 1)\}$	108
	$\oplus 9 \times \{(1, 1, \mathbf{3}) \oplus (1, 1, \bar{\mathbf{3}})\}$	54
	$\oplus 3 \times (1, \mathbf{8}_{v+c+s}, 1)$	72
	$\oplus 36 \times (1, 1, 1)$	36
	Supergravity singlets	2

TABLE IV. Exotic matter content in models 1A/B and 2 from [40]. Listed are the states' quantum numbers under the MSSM and hidden sector gauge groups, with the hypercharge denoted in the subscript. The brane-localized exotic matter in model 1 is a subset of that in model 2.

Model	Hidden sector		Exotic matter irrep.	Name
1 A/B	$SU(4) \times SU(2)$	Brane	$2 \times [(3, 1; 1, 1)_{1/3, 2/3} + (\bar{3}, 1; 1, 1)_{-1/3, -2/3}]$	$v + \bar{v}$
		Exotics	$4 \times [(1, 2; 1, 1)_{0,*} + (1, 2; 1, 1)_{0,*}]$	$m + m$
			$1 \times [(1, 2; 1, 2)_{0,0} + (1, 2; 1, 2)_{0,0}]$	$y + y$
			$2 \times [(1, 1; 4, 1)_{1,1} + (1, 1; \bar{4}, 1)_{-1,-1}]$	$f^+ + \bar{f}^-$
2	$SO(8) \times SU(2)$		$14 \times [(1, 1; 1, 1)_{1,*} + (1, 1; 1, 1)_{-1,*}]$	$s^+ + s^-$
		Bulk	$6 \times [(3, 1; 1, 1)_{-2/3, -2/3} + (\bar{3}, 1; 1, 1)_{2/3, 2/3}]$	$\delta + \bar{\delta}$
		Exotics	$1 \times [(3, 1; 1, 1)_{-2/3, -1/3} + (\bar{3}, 1; 1, 1)_{2/3, 1/3}]$	$d + \bar{d}$
			$1 \times [(1, 2; 1, 1)_{-1,-1} + (1, 2; 1, 1)_{1,1}]$	$\ell + \bar{\ell}$
		Brane	$4 \times [(3, 1; 1, 1)_{1/3,*} + (\bar{3}, 1; 1, 1)_{-1/3,*}]$	$v + \bar{v}$
		Exotics	$2 \times [(1, 2; 1, 1)_{0,*} + (1, 2; 1, 1)_{0,*}]$	$m + m$
			$1 \times [(1, 2; 1, 2)_{0,0} + (1, 2; 1, 2)_{0,0}]$	$y + y$
			$2 \times [(1, 1; 1, 2)_{1,1} + (1, 1; 1, 2)_{-1,-1}]$	$x^+ + x^-$
			$20 \times [(1, 1; 1, 1)_{1,*} + (1, 1; 1, 1)_{-1,*}]$	$s^+ + s^-$
		Bulk	$3 \times [(3, 1; 1, 1)_{-2/3, -2/3} + (\bar{3}, 1; 1, 1)_{2/3, 2/3}]$	$\delta + \bar{\delta}$
		Exotics	$1 \times [(3, 1; 1, 1)_{-2/3, 2/3} + (\bar{3}, 1; 1, 1)_{2/3, -2/3}]$	$d + \bar{d}$
			$1 \times [(1, 2; 1, 1)_{-1,-1} + (1, 2; 1, 1)_{1,1}]$	$\ell + \bar{\ell}$
			$3 \times [(1, 2; 1, 1)_{-1,0} + (1, 2; 1, 1)_{1,0}]$	$\phi + \bar{\phi}$

TABLE V. Values of the  $\beta$ -function coefficients for the brane-localized exotic matter. These states do not have zero modes and come from the  $T^3$  and  $T^1/T^5$  sectors of the theory.

Irrep.	Mult (model 2)	$b_3$	$b_2$	$b_Y$
$(3, 1)_{1/3} + (\bar{3}, 1)_{-1/3}$	4	1	0	1/10
$(1, 2)_0 + (1, 2)_0$	4	0	1	0
$(1, 1)_1 + (1, 1)_{-1}$	24	0	0	3/10

TABLE VI. Values of the  $\beta$ -function coefficients for matter living in the bulk, along with their embeddings into  $SU(6)$ . [The group branching rules for  $SU(6) \rightarrow SU(5) \times U(1)$  can be found in Ref. [57].] It is important to distinguish whether these are vector (V) or chiral (C) multiplets.

$SU(6)$ rep.		Irrep.	$b_3^{++}$	$b_2^{++}$	$b_Y^{++}$		Irrep.	$b_3^{--}$	$b_2^{--}$	$b_Y^{--}$
<b>35</b>	V	$(8, 1)_0$	-9	0	0	C	$(8, 1)_0$	3	0	0
	V	$(1, 3)_0$	0	-6	0	C	$(1, 3)_0$	0	2	0
	C	$(1, 2)_1$	0	1/2	3/10	V	$(1, 2)_{-1}$	0	-3/2	-9/10
	C	$(1, 2)_{-1}$	0	1/2	3/10	V	$(1, 2)_1$	0	-3/2	-9/10
<b>20</b>	C	$(3, 2)_{1/3}$	1	3/2	1/10	C	$(\bar{3}, 2)_{-1/3}$	1	3/2	1/10
	C	$(\bar{3}, 1)_{-4/3}$	1/2	0	4/5	C	$(3, 1)_{4/3}$	1/2	0	4/5
	C	$(1, 1)_2$	0	0	3/5	C	$(1, 1)_{-2}$	0	0	3/5
	C	$(1, 2)_{-1}$	0	1/2	3/10	C	$(1, 2)_1$	0	1/2	3/10
<b>6 + <math>\bar{6}</math></b>	C	$(\bar{3}, 1)_{2/3}$	1/2	0	1/5	C	$(3, 1)_{-2/3}$	1/2	0	1/5

TABLE VII. Comparison of proton lifetime to  $M_{\text{STRING}}$ ,  $M_C$ , and  $M_{\text{EX}}$ , in the case where no exotic matter lives in the bulk. In general, an intermediate scale is needed to fit the low-energy data and the proton decay constraints. We have used  $\beta_{\text{LATTICE}} \simeq 0.011$  [41]. We note the solutions which will also work for model 1A in bold. Note that  $\tilde{n}$  refers to brane-localized exotics only and is defined in Eq. (8).

$\tilde{n}$	$M_{\text{STRING}}$ in GeV	$M_C$ in GeV	$M_{\text{EX}}$ in GeV	$\tau(p \rightarrow e^+ \pi^0)$ in yr
<b>(2, 1, 0)</b>	<b><math>9.18 \times 10^{17}</math></b>	<b><math>2.22 \times 10^{17}</math></b>	<b><math>2.60 \times 10^9</math></b>	<b><math>1.77 \times 10^{38}</math></b>
(4, 2, 0)	$9.18 \times 10^{17}$	$2.22 \times 10^{17}$	$4.88 \times 10^{13}$	$1.77 \times 10^{38}$
(3, 2, 3)	$9.88 \times 10^{17}$	$2.22 \times 10^{17}$	$2.08 \times 10^9$	$1.32 \times 10^{38}$
(4, 3, 6)	$1.08 \times 10^{18}$	$2.22 \times 10^{17}$	$1.59 \times 10^9$	$9.23 \times 10^{37}$
(4, 2, 1)	$8.26 \times 10^{17}$	$6.65 \times 10^{16}$	$5.43 \times 10^{13}$	$2.19 \times 10^{36}$
(4, 2, 2)	$6.87 \times 10^{17}$	$2.19 \times 10^{16}$	$6.52 \times 10^{13}$	$5.34 \times 10^{34}$
<b>(2, 1, 1)</b>	<b><math>6.87 \times 10^{17}</math></b>	<b><math>2.19 \times 10^{16}</math></b>	<b><math>6.18 \times 10^9</math></b>	<b><math>5.34 \times 10^{34}</math></b>
(3, 2, 4)	$7.07 \times 10^{17}$	$2.16 \times 10^{16}$	$5.68 \times 10^9$	$4.52 \times 10^{34}$
(4, 3, 7)	$7.28 \times 10^{17}$	$2.13 \times 10^{16}$	$5.21 \times 10^9$	$3.79 \times 10^{34}$
(3, 1, 0)	$5.43 \times 10^{17}$	$8.20 \times 10^{15}$	$8.25 \times 10^{13}$	$2.70 \times 10^{33}$
(4, 2, 3)	$5.47 \times 10^{17}$	$8.15 \times 10^{15}$	$8.19 \times 10^{13}$	$2.57 \times 10^{33}$



TABLE VIII. Comparison of proton lifetime to  $M_{\text{STRING}}$ ,  $M_C$ , and  $M_{\text{EX}}$ . In general, an intermediate scale is needed to fit the low-energy data and the proton decay constraints. We have used  $\beta_{\text{LATTICE}} \simeq 0.011$  [41]. Note that  $\vec{n}$  refers to brane-localized exotics only and is defined in Eq. (8). For details on the solution marked with an arrow ( $\Rightarrow$ ), see Sec. IV. We note the solutions which will also work for model 1A in bold.

Bulk exotics	$\vec{n}$	$M_{\text{STRING}}$ in GeV	$M_{\text{C}}$ in GeV	$M_{\text{EX}}$ in GeV	$\tau(p \rightarrow e^+ \pi^0)$ in yr
$[(\mathbf{3}, 1)_{2/3,*} + (\bar{\mathbf{3}}, 1)_{-2/3,*}]^{++} + [(1, \mathbf{2})_{1,*} + (1, \mathbf{2})_{-1,*}]^{--}$	(4, 3, 1)	$9.96 \times 10^{17}$	$7.74 \times 10^{17}$	$4.50 \times 10^{13}$	$1.90 \times 10^{40}$
	(4, 3, 2)	$9.73 \times 10^{17}$	$2.22 \times 10^{17}$	$4.61 \times 10^{13}$	$1.40 \times 10^{38}$
	$\Rightarrow (\mathbf{2}, \mathbf{2}, \mathbf{2})$	$\mathbf{1.01 \times 10^{18}}$	$\mathbf{2.22 \times 10^{17}}$	$\mathbf{1.92 \times 10^9}$	$\mathbf{1.19 \times 10^{38}}$
	(3, 3, 5)	$1.12 \times 10^{18}$	$2.22 \times 10^{17}$	$1.43 \times 10^9$	$7.97 \times 10^{37}$
	(4, 4, 8)	$1.28 \times 10^{18}$	$2.22 \times 10^{17}$	$9.64 \times 10^8$	$4.73 \times 10^{37}$
	(3, 2, 0)	$8.79 \times 10^{17}$	$6.55 \times 10^{16}$	$5.10 \times 10^{13}$	$1.61 \times 10^{36}$
	(4, 3, 3)	$9.06 \times 10^{17}$	$6.50 \times 10^{16}$	$4.95 \times 10^{13}$	$1.38 \times 10^{36}$
	(3, 2, 1)	$7.67 \times 10^{17}$	$2.07 \times 10^{16}$	$5.84 \times 10^{13}$	$2.77 \times 10^{34}$
	$(\mathbf{1}, \mathbf{1}, \mathbf{0})$	$\mathbf{7.67 \times 10^{17}}$	$\mathbf{2.07 \times 10^{16}}$	$\mathbf{4.45 \times 10^9}$	$\mathbf{2.77 \times 10^{34}}$
	(4, 3, 4)	$7.82 \times 10^{17}$	$2.05 \times 10^{16}$	$5.73 \times 10^{13}$	$2.47 \times 10^{34}$
	$(\mathbf{2}, \mathbf{2}, \mathbf{3})$	$\mathbf{7.97 \times 10^{17}}$	$\mathbf{2.03 \times 10^{16}}$	$\mathbf{3.96 \times 10^9}$	$\mathbf{2.20 \times 10^{34}}$
	(3, 3, 6)	$8.31 \times 10^{17}$	$1.99 \times 10^{16}$	$3.50 \times 10^9$	$1.71 \times 10^{34}$
	(4, 4, 9)	$8.69 \times 10^{17}$	$1.95 \times 10^{16}$	$3.06 \times 10^9$	$1.31 \times 10^{34}$
	(4, 2, 0)	$6.69 \times 10^{17}$	$1.03 \times 10^{16}$	$1.44 \times 10^{15}$	$2.92 \times 10^{33}$
	$[(\mathbf{3}, 1)_{2/3,*} + (\bar{\mathbf{3}}, 1)_{-2/3,*}]^{--} + [(1, \mathbf{2})_{1,*} + (1, \mathbf{2})_{-1,*}]^{++}$	(3, 1, 1)	$1.01 \times 10^{18}$	$2.22 \times 10^{17}$	$1.92 \times 10^9$
(4, 2, 4)		$1.12 \times 10^{18}$	$2.22 \times 10^{17}$	$1.43 \times 10^9$	$7.97 \times 10^{37}$
(4, 1, 0)		$7.67 \times 10^{17}$	$2.07 \times 10^{16}$	$5.84 \times 10^{13}$	$2.77 \times 10^{34}$
(3, 1, 2)		$7.97 \times 10^{17}$	$2.03 \times 10^{16}$	$3.96 \times 10^9$	$2.20 \times 10^{34}$
(4, 2, 5)		$8.31 \times 10^{17}$	$1.99 \times 10^{16}$	$3.50 \times 10^9$	$1.71 \times 10^{34}$
$[(\mathbf{3}, 1)_{2/3,*} + (\bar{\mathbf{3}}, 1)_{-2/3,*}]^{++} + [(1, \mathbf{2})_{1,*} + (1, \mathbf{2})_{-1,*}]^{++}$	$(\mathbf{2}, \mathbf{1}, \mathbf{0})$	$\mathbf{1.01 \times 10^{18}}$	$\mathbf{2.22 \times 10^{17}}$	$\mathbf{1.92 \times 10^9}$	$\mathbf{1.19 \times 10^{38}}$
	(3, 2, 3)	$1.12 \times 10^{18}$	$2.22 \times 10^{17}$	$1.43 \times 10^9$	$7.97 \times 10^{37}$
	(4, 2, 0)	$9.73 \times 10^{17}$	$2.22 \times 10^{17}$	$4.61 \times 10^{13}$	$1.40 \times 10^{38}$
	(4, 3, 6)	$1.28 \times 10^{18}$	$2.22 \times 10^{17}$	$9.64 \times 10^8$	$4.73 \times 10^{37}$
	(4, 2, 1)	$9.06 \times 10^{17}$	$6.50 \times 10^{16}$	$4.95 \times 10^{13}$	$1.38 \times 10^{36}$
	(4, 2, 2)	$7.82 \times 10^{17}$	$2.05 \times 10^{16}$	$5.73 \times 10^{13}$	$2.47 \times 10^{34}$
	$(\mathbf{2}, \mathbf{1}, \mathbf{1})$	$\mathbf{7.97 \times 10^{17}}$	$\mathbf{2.03 \times 10^{16}}$	$\mathbf{3.96 \times 10^9}$	$\mathbf{2.20 \times 10^{34}}$
	(3, 2, 4)	$8.31 \times 10^{17}$	$1.99 \times 10^{16}$	$3.50 \times 10^9$	$1.71 \times 10^{34}$
	(4, 3, 7)	$8.69 \times 10^{17}$	$1.95 \times 10^{16}$	$3.06 \times 10^9$	$1.31 \times 10^{34}$
$[(\mathbf{3}, 1)_{2/3,*} + (\bar{\mathbf{3}}, 1)_{-2/3,*}]^{--} + [(1, \mathbf{2})_{1,*} + (1, \mathbf{2})_{-1,*}]^{--}$	$(\mathbf{2}, \mathbf{1}, \mathbf{0})$	$\mathbf{9.36 \times 10^{17}}$	$\mathbf{2.22 \times 10^{17}}$	$\mathbf{2.45 \times 10^9}$	$\mathbf{1.64 \times 10^{38}}$
	(4, 2, 0)	$9.36 \times 10^{17}$	$2.22 \times 10^{17}$	$4.79 \times 10^{13}$	$1.64 \times 10^{38}$
	(3, 2, 3)	$1.01 \times 10^{18}$	$2.22 \times 10^{17}$	$1.92 \times 10^9$	$1.19 \times 10^{38}$
	(4, 3, 6)	$1.12 \times 10^{18}$	$2.22 \times 10^{17}$	$1.43 \times 10^9$	$7.97 \times 10^{37}$
	(4, 2, 1)	$8.79 \times 10^{17}$	$6.55 \times 10^{16}$	$5.10 \times 10^{13}$	$1.61 \times 10^{36}$
	$(\mathbf{2}, \mathbf{1}, \mathbf{1})$	$\mathbf{7.67 \times 10^{17}}$	$\mathbf{2.07 \times 10^{16}}$	$\mathbf{4.45 \times 10^9}$	$\mathbf{2.77 \times 10^{34}}$
	(4, 2, 2)	$7.67 \times 10^{17}$	$2.07 \times 10^{16}$	$5.84 \times 10^{13}$	$2.77 \times 10^{34}$
	(3, 2, 4)	$7.97 \times 10^{17}$	$2.03 \times 10^{16}$	$3.96 \times 10^9$	$2.20 \times 10^{34}$
	(4, 3, 7)	$8.31 \times 10^{17}$	$1.99 \times 10^{16}$	$3.50 \times 10^9$	$1.71 \times 10^{34}$

TABLE IX. Subset of models listed in Tables VII and VIII which exhibit moderate hierarchies between all of the scales in the problem, as pictured in Fig. 5, in the red box. Note that none of these results can be accommodated in model 1A.

Bulk exotics	$\vec{n}$	$M_{\text{STRING}}$ in GeV	$M_C$ in GeV	$M_{\text{EX}}$ in GeV	$\tau(p \rightarrow e^+ \pi^0)$ in yr
None	(4, 2, 3)	$5.47 \times 10^{17}$	$8.15 \times 10^{15}$	$8.19 \times 10^{13}$	$2.57 \times 10^{33}$
	(3, 1, 0)	$5.43 \times 10^{17}$	$8.20 \times 10^{15}$	$8.25 \times 10^{13}$	$2.70 \times 10^{33}$
	(4, 2, 2)	$6.87 \times 10^{17}$	$2.19 \times 10^{16}$	$6.52 \times 10^{13}$	$5.34 \times 10^{34}$
$[(\mathbf{3}, 1)_{2/3,*} + (\bar{\mathbf{3}}, 1)_{-2/3,*}]^{++} + [(1, \mathbf{2})_{1,*} + (1, \mathbf{2})_{-1,*}]^{--}$	(4, 2, 0)	$6.69 \times 10^{17}$	$1.03 \times 10^{16}$	$1.44 \times 10^{15}$	$2.92 \times 10^{33}$
	(4, 3, 4)	$7.82 \times 10^{17}$	$2.05 \times 10^{16}$	$5.73 \times 10^{13}$	$2.47 \times 10^{34}$
	(3, 2, 1)	$7.67 \times 10^{17}$	$2.07 \times 10^{16}$	$5.84 \times 10^{13}$	$2.77 \times 10^{34}$
	(4, 1, 0)	$7.67 \times 10^{17}$	$2.07 \times 10^{16}$	$5.84 \times 10^{13}$	$2.77 \times 10^{34}$
$[(\mathbf{3}, 1)_{2/3,*} + (\bar{\mathbf{3}}, 1)_{-2/3,*}]^{--} + [(1, \mathbf{2})_{1,*} + (1, \mathbf{2})_{-1,*}]^{++}$	(4, 2, 2)	$7.82 \times 10^{17}$	$2.05 \times 10^{16}$	$5.73 \times 10^{13}$	$2.47 \times 10^{34}$
$[(\mathbf{3}, 1)_{2/3,*} + (\bar{\mathbf{3}}, 1)_{-2/3,*}]^{--} + [(1, \mathbf{2})_{1,*} + (1, \mathbf{2})_{-1,*}]^{--}$	(4, 2, 2)	$7.67 \times 10^{17}$	$2.07 \times 10^{16}$	$5.84 \times 10^{13}$	$2.77 \times 10^{34}$

- [1] S. Dimopoulos, S. Raby, and F. Wilczek, *Phys. Rev. D* **24**, 1681 (1981).
- [2] S. Dimopoulos and H. Georgi, *Nucl. Phys.* **B193**, 150 (1981).
- [3] L. E. Ibanez and G. G. Ross, *Phys. Lett.* **105B**, 439 (1981).
- [4] N. Sakai, *Z. Phys. C* **11**, 153 (1981).
- [5] M. B. Einhorn and D. R. T. Jones, *Nucl. Phys.* **B196**, 475 (1982).
- [6] W. J. Marciano and G. Senjanović, *Phys. Rev. D* **25**, 3092 (1982).
- [7] R. Dermišek, A. Mafi, and S. Raby, *Phys. Rev. D* **63**, 035001 (2000).
- [8] H. Murayama and A. Pierce, *Phys. Rev. D* **65**, 055009 (2002).
- [9] V. S. Kaplunovsky, *Nucl. Phys.* **B307**, 145 (1988); **B382**, 436(E) (1992). The full version (plus corrections) can be found at arXiv:hep-th/9205070.
- [10] L. J. Dixon, V. Kaplunovsky, and J. Louis, *Nucl. Phys.* **B329**, 27 (1990).
- [11] L. J. Dixon, V. Kaplunovsky, and J. Louis, *Nucl. Phys.* **B355**, 649 (1991).
- [12] K. R. Dienes, *Phys. Rep.* **287**, 447 (1997).
- [13] L. J. Dixon, J. A. Harvey, C. Vafa, and E. Witten, *Nucl. Phys.* **B261**, 678 (1985).
- [14] L. J. Dixon, J. A. Harvey, C. Vafa, and E. Witten, *Nucl. Phys.* **B274**, 285 (1986).
- [15] J. D. Breit, B. A. Ovrut, and G. C. Segre, *Phys. Lett.* **158B**, 33 (1985).
- [16] L. E. Ibáñez, J. E. Kim, H. P. Nilles, and F. Quevedo, *Phys. Lett. B* **191**, 282 (1987).
- [17] L. E. Ibáñez, H. P. Nilles, and F. Quevedo, *Phys. Lett. B* **187**, 25 (1987).
- [18] L. E. Ibáñez, H. P. Nilles, and F. Quevedo, *Phys. Lett. B* **192**, 332 (1987).
- [19] J. A. Casas and C. Muñoz, *Phys. Lett. B* **214**, 63 (1988).
- [20] J. A. Casas, E. K. Katehou, and C. Muñoz, *Nucl. Phys.* **B317**, 171 (1989).
- [21] K. R. Dienes, E. Dudas, and T. Gherghetta, *Phys. Lett. B* **436**, 55 (1998).
- [22] K. R. Dienes, E. Dudas, and T. Gherghetta, *Nucl. Phys.* **B537**, 47 (1999).
- [23] Y. Kawamura, *Prog. Theor. Phys.* **105**, 999 (2001).
- [24] L. J. Hall and Y. Nomura, *Phys. Rev. D* **64**, 055003 (2001).
- [25] T. Asaka, W. Buchmüller, and L. Covi, *Phys. Lett. B* **523**, 199 (2001).
- [26] R. Contino, L. Pilo, R. Rattazzi, and E. Trincherini, *Nucl. Phys.* **B622**, 227 (2002).
- [27] R. Dermišek and A. Mafi, *Phys. Rev. D* **65**, 055002 (2002).
- [28] L. J. Hall and Y. Nomura, *Ann. Phys. (N.Y.)* **306**, 132 (2003).
- [29] H. D. Kim and S. Raby, *J. High Energy Phys.* **01** (2003) 056.
- [30] H. M. Lee, *Phys. Lett. B* **643**, 136 (2006).
- [31] W. M. Yao *et al.* (Particle Data Group), *J. Phys. G* **33**, 1 (2006).
- [32] T. Kobayashi, S. Raby, and R.-J. Zhang, *Phys. Lett. B* **593**, 262 (2004).
- [33] S. Förste, H. P. Nilles, P. K. S. Vaudrevange, and A. Wingerter, *Phys. Rev. D* **70**, 106008 (2004).
- [34] T. Kobayashi, S. Raby, and R.-J. Zhang, *Nucl. Phys.* **B704**, 3 (2005).
- [35] J. E. Kim and B. Kyae, *Phys. Rev. D* **77**, 106008 (2008).
- [36] W. Buchmüller, K. Hamaguchi, O. Lebedev, and M. Ratz, *Phys. Rev. Lett.* **96**, 121602 (2006).
- [37] W. Buchmüller, K. Hamaguchi, O. Lebedev, and M. Ratz, *Nucl. Phys.* **B785**, 149 (2007).
- [38] O. Lebedev *et al.*, *Phys. Rev. Lett.* **98**, 181602 (2007).
- [39] O. Lebedev *et al.*, *Phys. Lett. B* **645**, 88 (2007).
- [40] O. Lebedev *et al.*, *Phys. Rev. D* **77**, 046013 (2008).
- [41] Y. Aoki, C. Dawson, J. Noaki, and A. Soni, *Phys. Rev. D* **75**, 014507 (2007).
- [42] L. J. Hall, Y. Nomura, and D. R. Smith, *Nucl. Phys.* **B639**, 307 (2002).
- [43] T. Kobayashi and N. Ohtsubo, *Int. J. Mod. Phys. A* **9**, 87 (1994).
- [44] T. Kobayashi, H. P. Nilles, F. Ploger, S. Raby, and M. Ratz, *Nucl. Phys.* **B768**, 135 (2007).
- [45] P. Ko, T. Kobayashi, J.-h. Park, and S. Raby, *Phys. Rev. D* **76**, 035005 (2007).
- [46] M. B. Green and J. H. Schwarz, *Phys. Lett.* **149B**, 117 (1984).
- [47] E. Witten, *Phys. Lett.* **149B**, 351 (1984).
- [48] M. Dine, N. Seiberg, and E. Witten, *Nucl. Phys.* **B289**, 589 (1987).
- [49] A. Sagnotti, *Phys. Lett. B* **294**, 196 (1992).
- [50] M. Berkooz *et al.*, *Nucl. Phys.* **B475**, 115 (1996).
- [51] L. E. Ibáñez, D. Lust, and G. G. Ross, *Phys. Lett. B* **272**, 251 (1991).
- [52] L. E. Ibáñez and D. Lust, *Nucl. Phys.* **B382**, 305 (1992).
- [53] A. Hebecker and M. Trapletti, *Nucl. Phys.* **B713**, 173 (2005).
- [54] D. C. Lewellen, *Nucl. Phys.* **B337**, 61 (1990); A. Font, L. E. Ibáñez, and F. Quevedo, *Nucl. Phys.* **B345**, 389 (1990); P. Mayr, H. P. Nilles, and S. Stieberger, *Phys. Lett. B* **317**, 53 (1993); L. E. Ibáñez, *Phys. Lett. B* **318**, 73 (1993); K. R. Dienes and A. E. Faraggi, *Phys. Rev. Lett.* **75**, 2646 (1995); *Nucl. Phys.* **B457**, 409 (1995); P. Hořava and E. Witten, *Nucl. Phys.* **B460**, 506 (1996); K. R. Dienes, A. E. Faraggi, and J. March-Russell, *Nucl. Phys.* **B467**, 44 (1996); E. Witten, *Nucl. Phys.* **B471**, 135 (1996); J. Giedt, *Mod. Phys. Lett. A* **18**, 1625 (2003); J. Perkins *et al.*, *Phys. Rev. D* **75**, 026007 (2007).
- [55] S. Weinberg, *Phys. Lett.* **91B**, 51 (1980).
- [56] L. J. Hall, *Nucl. Phys.* **B178**, 75 (1981).
- [57] R. Slansky, *Phys. Rep.* **79**, 1 (1981).
- [58] D. R. T. Jones, *Phys. Rev. D* **25**, 581 (1982).
- [59] D. M. Ghilencea and S. Groot Nibbelink, *Classical Quantum Gravity* **20**, S495 (2003).
- [60] O. Lebedev *et al.*, available publicly at <http://www.th.physik.uni-bonn.de/nilles/Z6IIorbifold/>.
- [61] W. Buchmüller, C. Lüdeling, and J. Schmidt, *J. High Energy Phys.* **09** (2007) 113.
- [62] M. Bershadsky, K. A. Intriligator, S. Kachru, D. R. Morrison, V. Sadov, and C. Vafa, *Nucl. Phys.* **B481**, 215 (1996).
- [63] J. Hisano, arXiv:hep-ph/0004266.
- [64] M. L. Alciati, F. Feruglio, Y. Lin, and A. Varagnolo, *J. High Energy Phys.* **03** (2005) 054.
- [65] B. Dundee and S. Raby (work in progress).